Reviewer 1

In this very well written manuscript the authors discuss results of thoroughly planned and described chamber experiments on the browning of aerosol particles upon exposure to gaseous glyoxal. Seed aerosols consisted of ammonium sulfate, methylammonium sulfate, mixed ammonium/glycine sulfate, and sodium sulfate, and were exposed to glyoxal under different relative humidity conditions. The authors observe a 'reversible' browning of the aerosol particles, when two conditions are met: 1) dry chamber conditions (<5% RH), and 2) amine functionalities are present in seed particles. Furthermore, the authors try to quantify the contribution of the observed browning to global radiative forcing induced by secondary brown carbon and conclude that its contribution is negligible with < 1%. The findings are discussed very well and contribute significantly to the field. I have a few comments beside technical corrections that need to be addressed in a minor revision prior publication:

General comments:

1) The observation that the browning process appears to be reversible is discussed at several points throughout the manuscript. Indeed, the single-scattering albedo in Figure 1 starts to recover with declining glyoxal gas-phase concentration. However, the addition of water vapor results in a sudden recovery of the albedo back to the baseline. This effect could also be due to a dilution effect, as the absorption properties of glyoxal derived brown carbon is known to be highly concentration dependent. Could the authors comment on a potential dilution effect, especially of surface active brown carbon constituents?

This comment is very thought-provoking. As noted by the reviewer, albedo declines when glyoxal gas concentrations go down, even before the humidity is increased. This dependence of particle absorptivity on glyoxal gas concentrations suggests full reversibility of brown carbon formation under dry conditions, and there is no reason to assume that this relationship would change after humidification. We cannot rule out the contribution of a dilution effect, however, and have re-written this section of the manuscript to include this possibility. In addition, we have included some information from the literature on the likely amount of water present on these effloresced aerosol particles at 50% RH – no more than 2 monolayers of adsorbed water are expected to be present.

> "At *t* = 5:46 h (Figure 1), the chamber was humidified to 50% RH, a level which would not deliquesce the AS seeds (Biskos et al., 2006) but which may produce as many as 1-2 monolayers of adsorbed water at aerosol surfaces consisting of solid AS (Denjean et al., 2014;Romakkaniemi et al., 2001) or glyoxal reaction products. (Hawkins et al., 2014). Humidification to 50% RH caused significant changes to both the gas and aerosol phases. Glyoxal PTR-MS signals and aerosol albedo returned within a few minutes back to near-baseline levels, while the dried aerosol mass measured by SMPS jumped downward by 15%. The loss of gas-phase glyoxal, again without aerosol growth, suggests that water greatly accelerated glyoxal loss rates to the steel chamber walls. The simultaneous albedo recovery and SMPS mass loss indicate that humidification destroyed all brown carbon products that absorb 450 nm light, converting some fraction of them to gas-phase products. A proposed mechanism for this process is discussed

below. It is significant that no browning was observed in PILS-sampled aerosol at any point during experiment 1, presumably due to the same mechanisms occurring during wet sampling."

A later paragraph describes the proposed mechanism:

"Proposed chemical mechanisms for brown carbon production at AS particle surfaces are summarized in Schemes 1 and S1. Except for steps where new N-heterocyclic rings are formed, all processes are reversible. (Kampf et al., 2012) Thus, a reduction of gas-phase glyoxal concentrations will shift reversible reactions away from BrC back towards simple N-heterocycle products, which do not absorb 450 nm light. Humidification to 50% RH accelerates this shift by removing more glyoxal from the gas phase, and perhaps also by hydrolysis of double bonds and dilution effects (Rincón et al., 2010;Phillips and Smith, 2014, 2015)."

2) Non-reversibly formed brown carbon from glyoxal might anyways not be present in appreciable amounts, given the timescale available for their formation. Maybe it would benefit the paper to expand a corresponding discussion a little bit, e.g., in line 201, where the formation of light-absorbing double bonds is mentioned.

Imidazole ring formation in the glyoxal + AS system is thought to be irreversible (Kampf et al., 2012), so it is significant that we detect two imidazole ring products in the aerosol phase when glyoxal is added, and upon water addition we detect the release of formic acid to the gas phase. (Formic acid is irreversibly co-produced with imidazole as the C-C bond of glyoxal breaks.) The formation of reversible and irreversible products, both detected and proposed, are now shown in a new Scheme 1.

3) The control experiment utilizing sodium sulfate seed aerosol is very helpful. It not only confirms the involvement of amine species in the observed fast and reversible browning effect, but also that the CAPS and PAS measurements were not biased by gas-phase glyoxal. Which other measures have been taken to ensure artifact-free analysis?

The CAPS instrument automatically samples through a filter periodically in order to remove signals from any gases present that absorb at 450 nm. We increased the frequency of filter sampling corrections to every five minutes to minimize any potential effects from gas-phase absorbers. This information is included in section 2.1. PAS and CRD aerosol measurements were also periodically baselined through filters for similar reasons. This information has been added to the manuscript, as shown below. Periodic gaps in CRD and PAS data indicate when filter baselines were performed. As noted by the reviewer, the control experiment demonstrates that these filter baselines successfully eliminated potential interference in aerosol optical signals even when high concentrations of glyoxal gas were present.

"Aerosol particles were sampled via diffusion driers by Q-AMS (Aerodyne), CAPS-ssa (Aerodyne, 450 nm), SMPS (TSI), CRD (530 nm) (Ugelow et al., 2017), and photoacoustic spectrometers (PAS, 405 and 530 nm) (Ugelow et al., 2017), all of which were periodically baselined through filters to eliminate interferences by gas-phase species. "

Technical comments:

4) Figure 3: Could the x-axis be labeled with "Elapsed Time (h)" as in Figure 1?

We have changed the x-axis of this figure to show elapsed time since start of experiment, consistent with Figure 1. We have changed the label as suggested.

5) Line 91: Brackets could be removed.

We have removed them.

Comments on the Supporting Information:

6) Figure S1: Start of chamber illumination (red line) – Did I miss it or is not there?

It's not there. We've removed reference to cloud events and chamber illumination from this figure, since neither are included.

7) Figure S2: Please include axis labels; the molecular masses for m/z 119 in brackets should be 96+23;

True. We have added the H^+ adduct mass to the caption, which makes the masses of both ions more self-explanatory, so we have removed the erroneous mass addition explanation.

Is it common for AMS analysis that formic acid appears as a protonated species at m/z 47?

The release of formic acid from aerosol upon humidification in our experiments was detected by PTR-MS, so we know that formic acid is one of the compounds being formed in the aerosol during dry glyoxal reactions. However, it has not been conclusively demonstrated that the Q-AMS *m/z* 47 signal is in fact due to formic acid. This signal could also be due to a $CH_3O_2^+$ fragment from hydrated imidazole carboxyaldehyde or a host of other known products. We have changed the text to read "formic acid or a $CH_3O_2^+$ fragment".

8) Figure S3: Exponents of the wall loss rate should be superscript

We have fixed this formatting error.

9) Figures S3, S4, S6: Could the x-axis label be changed to "Elapsed Time (h)"?

We have made this change.

Reviewer 2

Summary and recommendation: In this study, De Haan et al. report on fast browning of ammonium sulfate (AS), AS/glycine and methylammonium sulfate (MeAS) aerosol particles under dry conditions when exposed to gas phase glyoxal. It is shown that this browning process is not accompanied by noticeable particle growth and that this is reversed when water vapor is added. Remarkably, dry methylammonium sulfate aerosol was found to brown 4 times more than dry AS aerosol, and deliquesced AS aerosol browns much less than dry AS aerosol. Lastly, the authors estimate the impact of these browning processes on global radiative forcing, concluding that its contribution might only be important on a regional scale under polluted conditions. The authors acquired a nice dataset with state-of-the-art instruments during their chamber experiments, which will contribute to our understanding of brown carbon formation in aerosol particles. However, I see several points in the manuscript, which need to be addressed before I can recommend its publication in ACP (as detailed below).

Major comments:

1) Figure 1 / L111f: I cannot follow the authors' explanation of the SMPS mass loss upon chamber humidification. There is no mass increase upon GX addition under low RH levels, indicating that GX uptake to particles should be rather low. This is also consistent with the authors' assumption that most GX goes to the walls during this time (L102). So, how can a mass loss of ~15% upon humidification then be explained by destruction of light-absorbing products formed through GX uptake? If there was only minimal uptake of GX, the particles should still consist mainly of AS. One factor that might be important here is the wall loss correction, as particle wall losses can significantly change upon RH increase. Did the authors consider this in their analysis?

A change in gas loss rates upon RH increase is likely, and this could cause loss of molecules from aerosol due to Henry's law equilibria. A change in physical particle wall loss rates with RH is unlikely, since all particle impacts with chamber walls are thought to be irreversible regardless of wetness. Even if both gas and particle loss rates were to increase with RH, however, this would cause a change in the slope of the SMPS mass data, not a downward jump as was observed. Instead, supported by 3 lines of evidence described below, we reason that 15% of the AS particle volume must have been converted by 30 min of reaction with glyoxal under dry conditions (with small amounts of adsorbed water) into reaction products of similar volume that could later break down into gas-phase species upon humidification. These evaporating gas-phase species include formic acid and acetic acid (whose release was detected by PTR-MS upon humidification in several large chamber experiments), and likely imidazole, ammonia, and a variety of imine species. Indeed, the aerosol-phase production of imidazole and other volatile C-N species was observed by Q-AMS during dry glyoxal exposure in several small chamber experiments, consistent with this explanation. In addition, the large changes in albedo upon glyoxal exposure also suggest that even though particle size was not changing, we should not equate this with a lack of glyoxal reactivity or uptake. The manuscript has been updated to make these arguments more clearly:

"The 15% aerosol mass loss upon humidification to 50% RH is surprising, given that no corresponding mass gain was recorded during exposure to glyoxal under dry conditions. However, the lack of mass gain under dry conditions cannot be interpreted as a lack of glyoxal uptake or reactivity, given the large observed drop in albedo. Instead, the mass loss upon humidification suggests that at least 15% of the volume of AS seeds had been replaced under dry conditions by glyoxal reaction products that could break down into gas phase species once water was added. Simultaneous increases in gas-phase PTR-MS signals for *m/z* 47 (formic acid) and 61 (acetic acid) indicate that these acids were two of the gas-phase products generated by humidification. Formic acid is a known byproduct of imidazole production by aqueous-phase glyoxal + ammonia reactions (De Haan et al., 2009;Yu et al., 2011)."

2) I think the manuscript would largely benefit from some reaction mechanisms. This would help non-expert readers a lot in grasping the chemistry behind the browning reactions / imidazole formation. In the current version, all details on known and hypothesized chemical pathways are rather "hidden" in the text.

We fully agree with this suggestion, and have added Schemes 1 and S1 to summarize known and proposed chemistry of this system. We have placed it in the text at the point where we first discuss the AMS detection of imidazoles in the dry AS aerosol after glyoxal addition:

"The detection of particle-phase imidazole, pyrazine, and IC suggests the presence of larger, light-absorbing molecules such as 2,2'-biimidazole and N-heterocycle derivatives that are typically associated with the products detected here. (Kampf et al., 2012;Hawkins et al., 2018;Grace et al., 2019) However, detection of the larger product molecules directly from dry aerosol may require a soft, direct ionization technique such as extractive electrospray ionization (EESI-) MS.

"Proposed chemical mechanisms for brown carbon production at AS particle surfaces are summarized in Schemes 1 and S1. Except for steps where new N-heterocyclic rings are formed, all processes are reversible. (Kampf et al., 2012) Thus, a reduction of gas-phase glyoxal concentrations will shift reversible reactions away from BrC back towards simple N-heterocycle products, which do not absorb 450 nm light. Humidification to 50% RH accelerates this shift by removing more glyoxal from the gas phase, and perhaps also by hydrolysis of double bonds and dilution effects (Rincón et al., 2010;Phillips and Smith, 2014, 2015). Humidification also triggers the observed evaporation of formate as formic acid, and perhaps the evaporation of other small N-containing products."

Here is Scheme 1:

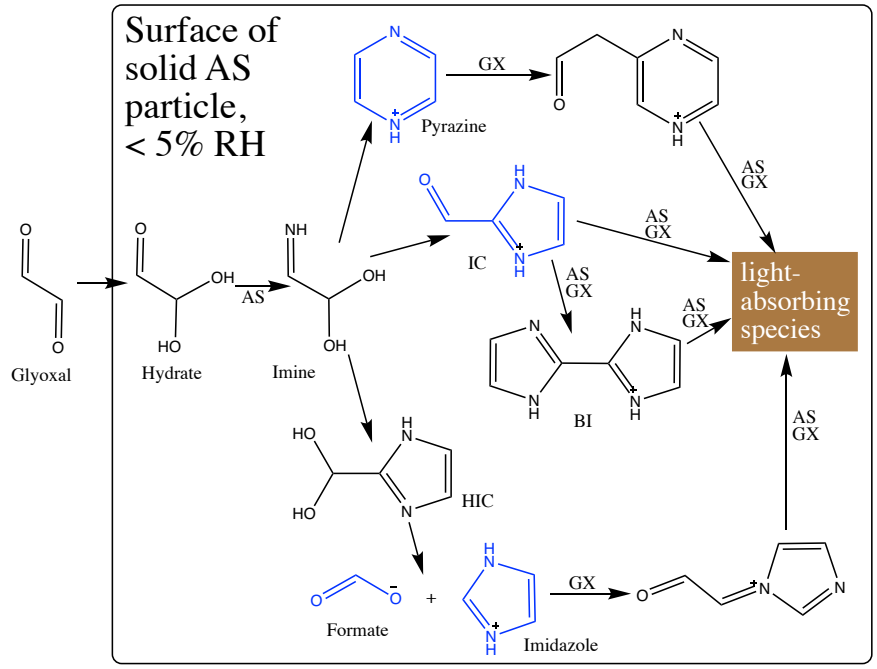

Scheme 1: Proposed brown carbon formation pathways of glyoxal reacting at solid AS aerosol particle surfaces. Products detected in this study are shown in blue. IC = 1H-imidazole-2-carboxaldehyde. BI = 2,2'-biimidazole (Kampf et al., 2012). AS = ammonium sulfate. GX = glyoxal. We assume, following (Kampf et al., 2012), that all reactions are reversible except for formation of N-heterocycle rings. See Scheme S1 for corresponding diagram of pathways under conditions of humidification.

3) The discussion section is extremely speculative. Especially, since RH conditions of < 5% are commonly far from tropospheric conditions. The mere statement that "tropospheric aerosol is nevertheless typically semi-solid or solid" (Line 212) does not eliminate this constraint. Therefore, I find it difficult to agree on the authors conclusion that aerosol browning by AS + GX under dry conditions may be regionally important.

This difference between dry chamber conditions and the troposphere is one of two reasons our estimation of the atmospheric significance of browning of sulfate aerosol by glyoxal is an upper limit. We have now explicitly stated our assumption, made for the purposes of the estimation, that ammonium sulfate aerosol in our *dry* chamber react the same way as tropospheric sulfate aerosol, as long as they are *solid* phase. If we are wrong in this (now explicitly stated) assumption, our upper limit will be too high – still an upper limit, but less useful. Since our estimated upper limit is already low enough that we can conclude that this browning process cannot be globally significant, the validity of this assumption does not impact the main conclusion of the paper. We have made the following revision to the text:

> "We will assume that all tropospheric sulfate particles contain ammonium, and, as an upper limit, that solid-phase tropospheric sulfate particles would brown as much as the pure, fully dry AS particles used in this study regardless of the presence of additional aerosol species. The first assumption is generally reasonable (Jimenez et al., 2009), since acidic sulfate aerosol takes up ammonia in the atmosphere, while the second assumption will clearly result in the estimation of an upper limit, since the presence of other materials at aerosol particle surfaces has been shown to limit the extent of the interactions between glyoxal and ammonium ions (Drozd and McNeill, 2014), and few locations in the troposphere are as dry as in this study. Tropospheric aerosol particles are typically semi-solid or solid phase, except low over the Amazon and Arctic (Shiraiwa et al., 2017)."

Specific comments:

1) L67 and L93f: How was the wall loss correction performed? It would be helpful to have some more details here.

Wall losses are calculated using size-dependent loss rates measured for AS test particles in the dry CESAM chamber. This information has been added to the manuscript in the Methods section 2.1:

> "SMPS size distributions were also corrected using size-dependent wall losses measured for AS particles in the chamber."

2) 2a) Figure 1 / L90: I would suggest to set t = 0 h for the GX addition to improve readability.

Regrettably, since the majority of experiments used gradual rather than pulsed glyoxal additions, and since experiment 1 used two glyoxal pulses, we would not be able to have a consistent time axis – as requested by the other two reviewers – if we used this suggestion.

2b) Figure 1: unit of aerosol density is missing in the caption

We have added the units, "g/cm^3", to the caption.

3) L124 / Figure S1: The strong difference between the experiments with AS and AS/glycine seeds needs a more detailed discussion. Only referring to differences in volatility without further discussion seems too vague.

We have added an additional line of reasoning to this section where we discuss the apparent lack of volatility of glyoxal + glycine reaction products upon water addition:

> "This may be due to the lower volatility of deprotonated seed particle materials (glycine vs. ammonia). In addition, most glycine-derivatized imidazole products have permanent positive charges and are not in equilibrium with volatile neutral forms (De Haan et al., 2009)."

4) Table 1 and corresponding figures: It is not reasonable to assume a density of 1 g/cm3 for the seed particles. Please use some more realistic numbers.

Once glyoxal reactions begin, particle densities are no longer certain. However, the densities of the aerosol seeds are known, and so we have added this information to Table 1. We have also corrected the seed aerosol concentrations listed in Table 1 that are based on SMPS measurements, which therefore depend on these densities. Since the seed aerosol concentrations are listed in Table 1 at the point of the start of glyoxal addition, the density cannot yet have changed, and so these numbers should be fully accurate. We have also corrected the SMPS masses in both figures that show such data (Figures 1 and S1) using seed particle densities, and note these densities in the captions of these figures.

5) Figure S2: Axis labels are missing.

We have added axis labels.

5) Line 129f: Are these increases in AMS ion signals significant? Would it be possible to give some more quantitative information here? Otherwise, it is not possible to judge whether this is an important contribution to the composition of the particles. Furthermore, is the resolution of a Q-AMS sufficient to assign all these signals unambiguously to certain compounds and corresponding fragments?

The increases described here are changes in averaged signals of at least +30% relative to conserved aerosol species such as sulfate ions, whose random variation when averaged signals are compared is always less than 10%. The data is shown visually in Figure S2. We have edited the manuscript to read:

> "A marginal (0.9 μg/m^3, S/N = 1.6) increase in total organic aerosol was observed by Q-AMS during glyoxal addition, associated with significant increases (+30% or more relative to conserved aerosol species) in ion signals at *m/z* 15 (CH_3^+ or NH^+ fragments), 23 (Na^+), 29 (CHO^+ fragment), 47 (formic acid+H^+ or a $CH_3O_2^+$ fragment), 69 (imidazole-H^+), 81 (pyrazine-H^+), 97 and 119 (imidazole carboxyaldehyde "IC" +H^+ and Na^+, respectively). Slight decreases in aerosol water signals were observed at *m/z* 16. "

Q-AMS does not permit unambiguous assignments. However, the glyoxal + AS system has been studied enough by high-resolution AMS that the identities of major peaks are known. We have changed the assignment of *m/z* 47 from "formic acid" to "formic acid+H^+ or a $CH_3O_2^+$ fragment" throughout the manuscript and supplement, since this assignment is ambiguous.

7) Why are experiments 8 and 9 discussed before experiment 5–7? I would suggest to rename the experiments or to reorganize the manuscript.

We have renumbered the experiments so that they are now referred to in order.

8) Figures 3, S3, S4, and S6: I would suggest using a relative time on the x-axis instead of the time of the day. This would improve readability. Moreover, it would be consistent with Figure 1.

We have made this change to Figure 3. For the figures in the supplement, we have changed the time axis label to "Elapsed Time (h)"

9) It would be nice to see at least for one of the experiments on wet AS an experimental overview figure (e.g., in the supplement) in the style of Fig. 1. Currently, the reader has to imagine how the experimental procedure and corresponding data looked like.

We now show a new summary overview figure for experiment 7 (wet AS) in the SI section, Figure S8. This is the highest RH experiment, and shows that the albedo change of -0.012 upon glyoxal addition is easily measurable by CAPS at 450 nm.

10) With a logarithmic y axis it should be possible to show both curves in one figure.

I am not sure which curves and which figure this comment refers to.

11) Table 1, experiment 1b: How did the authors infer a decrease of 3 µg/m3? From Fig. 1 the decrease seems to be in the range of 8–10 µg/m3. Moreover, this is inconsistent with the authors' statement (L111), that a mass decrease of ∼15% was observed.

The mass decrease of 3 µg/m3 listed in Table 1 for experiment 1b is the SMPS mass loss observed over 30 minutes after 0.50 ppm glyoxal was added. We have changed the Table 1 column label from "mass increase" to "mass increase upon glyoxal addition". The 8-10 µg/m3 mass loss in Figure 1 that the reviewer refers to is what was observed when the chamber was humidified to 50% RH. This value is not included in Table 1 because the chamber was rapidly humidified from <5 to 50% RH only in experiments 1b and 2.

Technical comments:

1) L95: I guess this should read "lack of uptake".
   Corrected.
2) Caption of Table 1: The ± sign should be formatted in black.
   Corrected.

Reviewer 3

Summary and recommendation: This paper details experiments the production of brown-carbon formation and light scattering ability as a function of relative humidity and minor chemical differences in aerosol type. The authors find that dry particles produce larger albedo changes upon introduction of glyoxal into their chamber than for wet particles. They also connect relative humidity changes to albedo and particle mass measurements and explain these results in the context of global radiative forcing impact, which may hold local significance even if not globally significant. In general, the results are clearly presented, the conclusions well thought out, and offer meaningful contributions to the field at large. I believe there are, however, several points that the authors need to clarify before acceptance for publication to better articulate the impact of the work.

Major comments:

1. In Table 1 is appears that reactions 1a and 3 are nearly identical with the exception of chamber. The results, as given by aerosol concentration, mass increase, and albedo change, however, and markedly different. Is the only difference here the chamber used? It is not clear from the text how the reader should understand these differing results. The authors would do to clarify how the two chambers affect their results and offer some guidance on how their results should be read in light of those differences.

Author response: The major difference between experiments 1a and 3 are that in experiment 1a, glyoxal was added in a pulse, and created a small, short-lived optical signal in the CAPS instrument, which is well-suited to measuring sudden changes in optical parameters. In experiment 3, glyoxal was added continuously over 25 minutes to reach the same concentration, and was therefore not detectable by CAPS. In both experiments, no increase in particle diameter was detectable by SMPS. However, experiment 3 also had AMS monitoring, which recorded a barely-measurable 0.9 ug/m3 increase in organic aerosol (S/N = 1.6). The manuscript has been edited to clarify these differences:

> "To better understand the reactive processes happening in the dry aerosol particles, further experiments were conducted in a 300 L Tedlar chamber probed by Q-AMS, SMPS, CAPS-ssa, and CRD/PAS. Figure S2 shows an AMS ion correlation plot comparing signals before and after 40 ppb glyoxal was added over a period of 25 minutes to the dry chamber containing AS aerosol in experiment 3. Unsurprisingly, the gradual addition of this smaller amount of glyoxal did not cause observable net particle growth or a decline in aerosol albedo at 450 nm. A marginal (0.9 $\mu g/m^3$, S/N = 1.6) increase in total organic aerosol was observed by Q-AMS during glyoxal addition, associated with increases in ion signals at *m/z* 15 (CH_3^+ or NH^+ fragments), 23 (Na^+), 29 (CHO^+ fragment), 47 (formic acid+H^+ or a $CH_3O_2^+$ fragment), 69 (imidazole-H^+), 81 (pyrazine-H^+), 97 and 119 (imidazole carboxyaldehyde "IC" +H^+ and Na^+, respectively), while slight decreases in aerosol water signals were observed at *m/z* 16"

2. In lines 95-99 the authors make the case that the lack of particle growth is consistent with a lack of uptake of glyoxal at low RH, but in lines 195-196, the possible (though small) uptake of glyoxal is highlighted as a reason for water depletion. If the results suggest that glyoxal is able to access surface water (and thus uptake to the particle even under dry conditions), shouldn't this be taken into account in the particle growth discussion?

We have edited line 95-96 to remove the comment about uptake, since what we were trying to point out is that the lack of observed growth under dry conditions was consistent with earlier studies. In this work, however, our chemical and optical measurements suggest that the lack of growth does NOT indicate a lack of glyoxal uptake or reactivity. Instead, they suggest that glyoxal is converting a fraction of the AS particles into brown carbon reaction products without a net gain in volume. We now try to make this distinction clear from the outset of the results section. This section now reads:

> "This lack of observed growth at <5% RH is consistent with previous studies under very dry conditions (Kroll et al., 2005;De Haan et al., 2017). However, as optical and chemical measurements described below will show, this lack of growth does not indicate a lack of glyoxal reactivity."

3. Following on to point #2, in lines 102-104 the discussion is hard to follow. The loss of glyoxal is largely to the steel walls, and yet the large albedo decline is also due to glyoxal-driven surface reactions? Does this suggest that even minor amounts of reactivity lead to very high albedo changes? I think the confusion readers will have with this section that the authors need to clear up is related to the sizing language. How should we read "largely", "large", and "at least some" in order to understand the weight of the argument the authors are making here?

We have re-written this section to try to avoid ambiguity and confusion. The rapid drop in albedo indicates rapid particle-phase brown carbon formation, which is followed by a much slower loss of glyoxal to the chamber walls. This paragraph now discusses these two events in order:

> "The addition of 0.05 ppm glyoxal gas at t = 4:47 h triggered a short-lived drop in albedo by 0.034 that was observed by CAPS-ssa at 450 nm. A second, larger glyoxal addition (0.50 ppm) at t = 5:16 h caused albedo to plummet to 0.75, a change 7× greater than the first. Even though particle sizes did not increase after either glyoxal addition, the significant albedo declines indicate that glyoxal reactions rapidly produced light-absorbing products at dry AS particle surfaces. Over the next 30 minutes, as glyoxal gas-phase concentrations decreased by half (likely to due to chamber wall losses), aerosol albedo recovered proportionately, indicating that this surface brown carbon formation under dry conditions is fully reversible."

4. In regards to Figure 1, how much of the recovery of albedo upon introduction of water is due to exclusively to the introduction of the water and how much is due to there still being glyoxal in the chamber as evidenced by the PTR-MS signals at 59 and 31? Unlike the earlier addition of a small glyoxal concentration, this larger addition was not allowed to return to

baseline, and while this may not matter in the resultant albedo recovery upon water addition discussion, this overlap isn't addressed adequately in the text. Essentially, is the albedo increase due to the addition of the water, or the resultant dilution/loss of glyoxal signal?

Since loss of glyoxal caused a loss of brown carbon for the previous 30 minutes without water addition, this mechanism is presumably still in play when water addition causes most of the remaining glyoxal to be removed from the gas phase (likely due to rapid wall losses). However, we cannot rule out an additional contribution from water, due either to dilution effects (suggested by Reviewer 1) or hydrolysis of brown carbon products. We have added a new paragraph that discusses the mechanisms of brown carbon formation and removal upon humidification:

> "Proposed chemical mechanisms for brown carbon production at AS particle surfaces are summarized in Schemes 1 and S1. Except for steps where new N-heterocyclic rings are formed, all processes are reversible (Kampf et al., 2012). Thus, a reduction of gas-phase glyoxal concentrations will shift reversible reactions away from BrC back towards simple N-heterocycle products, which do not absorb 450 nm light. Humidification to 50% RH accelerates this shift by removing more glyoxal from the gas phase, and perhaps also by hydrolysis of double bonds and dilution effects (Rincón et al., 2010;Phillips and Smith, 2014, 2015)."

5. In lines 143-144, and Figure 2 the case is made for albedo change as a function of glyoxal concentration being a second order polynomial with respect to glyoxal concentration. Is there a physical explanation that would help defend this choice, or is it simply what fit the data? Or, is there a reason that using a two-slope approach (say a linear fit to the data at [glyoxal] < 0.35 ppm and another linear fit to the data at [glyoxal] > 0.35 ppm) wouldn't also successfully capture the data? The authors should offer with what significance the readers should approach this polynomial fit and [gly]^2 dependence.

Since imidazole formation requires two glyoxal molecules, it is reasonable that the production of imidazole-based brown carbon is second order with respect to glyoxal concentrations. Furthermore, the kinetics of glyoxal + NH4+ are known to be concentration dependent, as determined by Noziere *et al.* (Noziere et al., 2009) We have added the following sentence justifying the curvature in Figure 2 to the manuscript:

> "While glyoxal + ammonium reactions are 1st order in glyoxal in dilute solution when [glyoxal] × [NH_4^+] < 1.2 M, they switch to 2nd order at higher concentrations (Noziere et al., 2009), which are likely in adsorbed surface water environments in these dry experiments."

Minor and technical comments:

1. At least when I downloaded a copy of the paper, Table 1 had some jumbled values in the last column (it would appear that those values are line numbers). The authors should check this Table to ensure that everything is in the place they expect it to be. This could very well be an artifact of the download and not the paper, and so this might disappear in final publication.

This appears to have been a function of the pdf conversion. We will pay attention to this.

2. In regards to the discussion on lines 195-196 again, a more curiosity-driven question the authors may consider, if they wish, commenting on is: can this ability of glyoxal to access surface water lead to a localized area of highly concentrated glyoxal (and that would thus accelerate chemical reactivity)?

Yes, in our opinion the evidence points in this direction. As described earlier, the kinetics of this reaction are concentration dependent, and in this study the kinetics clearly match high concentration conditions. We have added this idea to the discussion of Figure 2:

> "While glyoxal + ammonium reactions are 1st order in glyoxal in dilute solution when [glyoxal] × [NH_4^+] < 1.2 M, they switch to 2nd order at higher concentrations,(Noziere et al., 2009) which are likely in adsorbed surface water environments in these dry experiments."

We explain this concept in more detail at the end of the Results section:

> "Any adsorbed water would be saturated with ammonium (or methylammonium) sulfate, and the presence of dissolved AS is known to greatly increase glyoxal uptake via a "salting in" effect (Kampf et al., 2013;Waxman et al., 2015), while methylglyoxal solubility is reduced by salting out (Waxman et al., 2015). Thus, both reactants are expected to be concentrated in any surface-adsorbed water present. In a previous study, similar reasoning was used to explain glyoxal uptake on solid seed particles at RH levels as low as 10% (Corrigan et al., 2008). Furthermore, the scarcity of water will favor dehydration of products, helping to form light-absorbing conjugated double bonds."

References cited:

Biskos, G., Paulsen, D., Russell, L. M., Buseck, P. R., and Martin, S. T.: Prompt deliquescence and efflorescence of aerosol nanoparticles, Atmos. Chem. Phys., 6, 4633-4642, 10.5194/acp-6-4633-2006, 2006.

Corrigan, A. L., Hanley, S. W., and De Haan, D. O.: Uptake of glyoxal by organic and inorganic aerosol, Environ. Sci. Technol., 42, 4428-4433, 10.1021/es7032394, 2008.

De Haan, D. O., Corrigan, A. L., Smith, K. W., Stroik, D. R., Turley, J. T., Lee, F. E., Tolbert, M. A., Jimenez, J. L., Cordova, K. E., and Ferrell, G. R.: Secondary organic aerosol-forming reactions of glyoxal with amino acids, Environ. Sci. Technol., 43, 2818-2824, 10.1021/es803534f, 2009.

De Haan, D. O., Hawkins, L. N., Welsh, H. G., Pednekar, R., Casar, J. R., Pennington, E. A., de Loera, A., Jimenez, N. G., Symons, M. A., Zauscher, M., Pajunoja, A., Caponi, L., Cazaunau, M., Formenti, P., Gratien, A., Pangui, E., and Doussin, J. F.: Brown carbon production in ammonium- or amine-containing aerosol particles by reactive uptake of methylglyoxal and photolytic cloud cycling, Environ Sci Technol, 51, 7458-7466, 10.1021/acs.est.7b00159, 2017.

Denjean, C., Formenti, P., Picquet-Varrault, B., Katrib, Y., Pangui, E., Zapf, P., and Doussin, J. F.: A new experimental approach to study the hygroscopic and optical properties of aerosols: application to ammonium sulfate particles, Atmos. Meas. Tech., 7, 183-197, 10.5194/amt-7-183-2014, 2014.

Drozd, G. T., and McNeill, V. F.: Organic matrix effects on the formation of light-absorbing compounds from [small alpha]-dicarbonyls in aqueous salt solution, Environmental Science: Processes & Impacts, 16, 741-747, 10.1039/C3EM00579H, 2014.

Grace, D. N., Sharp, J. R., Holappa, R. E., Lugos, E. N., Sebold, M. B., Griffith, D. R., Hendrickson, H. P., and Galloway, M. M.: Heterocyclic Product Formation in Aqueous Brown Carbon Systems, ACS Earth and Space Chemistry, 3, 2472-2481, 10.1021/acsearthspacechem.9b00235, 2019.

Hawkins, L. N., Baril, M. J., Sedehi, N., Galloway, M. M., De Haan, D. O., Schill, G. P., and Tolbert, M. A.: Formation of semi-solid, oligomerized aqueous SOA: Lab simulations of cloud processing, Environ Sci Technol, 48, 2273-2280, 10.1021/es4049626, 2014.

Hawkins, L. N., Welsh, H. G., and Alexander, M. V.: Evidence for pyrazine-based chromophores in cloud water mimics containing methylglyoxal and ammonium sulfate, Atmos. Chem. Phys., 18, 12413-12431, 10.5194/acp-18-12413-2018, 2018.

Jimenez, J. L., Canagaratna, M. R., Donahue, N. M., Prevot, A. S. H., Zhang, Q., Kroll, J. H., DeCarlo, P. F., Allan, J. D., Coe, H., Ng, N. L., Aiken, A. C., Docherty, K. S., Ulbrich, I. M., Grieshop, A. P., Robinson, A. L., Duplissy, J., Smith, J. D., Wilson, K. R., Lanz, V. A., Hueglin, C., Sun, Y. L., Tian, J., Laadsonen, A., Raatikainen, T., Rautiainen, J., Vaattovaara, P., Ehn, M., Kulmala, M., Tomlinson, J. M., Collins, D. R., Cubison, M. J., Dunlea, E. J., Huffman, J. A., Onasch, T. B., Alfarra, M. R., Williams, P. I., Bower, K., Kondo, Y., Schneider, J., Drewnick, F., Borrmann, S., Weimer, S., Demerjian, K., Salcedo, D., Cottrell, L., Griffin, R., Takami, A., Miyoshi, T., Hatakeyama, S., Shimono, A., Sun, J. Y., Zhang, Y. M., Dzepina, K., Kimmel, J. R., Sueper, D., Jayne, J. T., Herndon, S. C., Trimborn, A. M., Williams, L. R., Wood, E. C., Middlebrook, A. M., Kolb, C. E., Baltensperger, U., and Worsnop, D. R.: Evolution of organic aerosols in the atmosphere, Science, 326, 1525-1529, 10.1126/science.1180353, 2009.

Kampf, C. J., Jakob, R., and Hoffmann, T.: Identification and characterization of aging products in the glyoxal/ammonium sulfate system -- implications for light-absorbing material in atmospheric aerosols, Atmos. Chem. Phys., 12, 6323-6333, 10.5194/acp-12-6323-2012, 2012.

Kampf, C. J., Waxman, E. M., Slowik, J. G., Dommen, J., Pfaffenberger, L., Praplan, A. P., Prévôt, A. S. H., Baltensperger, U., Hoffmann, T., and Volkamer, R.: Effective Henry's Law Partitioning and the Salting Constant of Glyoxal in Aerosols Containing Sulfate, Environ Sci Technol, 47, 4236-4244, 10.1021/es400083d, 2013.

Kroll, J. H., Ng, N. L., Murphy, S. M., Varutbangkul, V., Flagan, R. C., and Seinfeld, J. H.: Chamber studies of secondary organic aerosol growth by reactive uptake of simple carbonyl compounds, J. Geophys. Res., 110, D23207, 10.1029/2005jd006004, 2005.

Noziere, B., Dziedzic, P., and Cordova, A.: Products and kinetics of the liquid-phase reaction of glyoxal catalyzed by ammonium ions (NH_4^+), J. Phys. Chem., 113, 231-237, 10.1021/jp8078293, 2009.

Phillips, S. M., and Smith, G. D.: Light absorption by charge transfer complexes in brown carbon aerosols, Environ. Sci. Technol. Lett., 1, 382-386, 10.1021/ez500263j, 2014.

Phillips, S. M., and Smith, G. D.: Further evidence for charge transfer complexes in brown carbon aerosols from excitation-emission matrix fluorescence spectroscopy, J. Phys. Chem., 119, 4545-4551, 10.1021/jp510709e, 2015.

Rincón, A. G., Guzmán, M. I., Hoffmann, M. R., and Colussi, A. J.: Thermochromism of model organic aerosol matter, J. Phys. Chem. Lett., 1, 368-373, 10.1021/jz900186e 2010.

Romakkaniemi, S., Hämeri, K., Väkevä, M., and Laaksonen, A.: Adsorption of Water on 8−15 nm NaCl and (NH4)2SO4 Aerosols Measured Using an Ultrafine Tandem Differential Mobility Analyzer, The Journal of Physical Chemistry A, 105, 8183-8188, 10.1021/jp010647l, 2001.

Shiraiwa, M., Li, Y., Tsimpidi, A. P., Karydis, V. A., Berkemeier, T., Pandis, S. N., Lelieveld, J., Koop, T., and Pöschl, U.: Global distribution of particle phase state in atmospheric secondary organic aerosols, Nature Communications, 8, 15002, 10.1038/ncomms15002, 2017.

Ugelow, M. S., Zarzana, K. J., Day, D. A., Jimenez, J. L., and Tolbert, M. A.: The optical and chemical properties of discharge generated organic haze using in-situ real-time techniques, Icarus, 294, 1-13, https://doi.org/10.1016/j.icarus.2017.04.028, 2017.

Waxman, E. M., Elm, J., Kurtén, T., Mikkelsen, K. V., Ziemann, P. J., and Volkamer, R.: Glyoxal and Methylglyoxal Setschenow Salting Constants in Sulfate, Nitrate, and Chloride Solutions: Measurements and Gibbs Energies, Environ Sci Technol, 49, 11500-11508, 10.1021/acs.est.5b02782, 2015.

Yu, G., Bayer, A. R., Galloway, M. M., Korshavn, K. J., Fry, C. G., and Keutsch, F. N.: Glyoxal in aqueous ammonium sulfate solutions: products, kinetics, and hydration effects, Environ. Sci. Technol., 45, 6336-6342, 10.1021/es200989n, 2011.

Glyoxal's impact on dry ammonium salts: fast and reversible surface aerosol browning

David O. De Haan,*[1] Lelia N. Hawkins,[2] Kevin Jansen,[3] Hannah G. Welsh,[2] Raunak Pednekar,[2,5] Alexia de Loera,[1] Natalie G. Jimenez,[1] Margaret A. Tolbert,[3] Mathieu Cazaunau,[4] Aline Gratien,[4] Antonin Bergé,[4] Edouard Pangui,[4] Paola Formenti,[4] Jean-François Doussin[4]

[1] Department of Chemistry and Biochemistry, University of San Diego, 5998 Alcala Park, San Diego CA 92110 USA
[2] Department of Chemistry, Harvey Mudd College, 301 Platt Blvd, Claremont CA 91711 USA
[3] Department of Chemistry / Cooperative Institute for Research in Environmental Sciences, University of Colorado, Boulder CO 80309 USA
[4] Laboratoire Interuniversitaire des Systèmes Atmosphériques (LISA), UMR7583, CNRS, Université Paris-Est-Créteil (UPEC) et Université de Paris, Institut Pierre Simon Laplace (IPSL), Créteil, France
[5] Deceased

Correspondence to: David O. De Haan (ddehaan@sandiego.edu)

Abstract. Alpha-dicarbonyl compounds are believed to form brown carbon in the atmosphere via reactions with ammonium sulfate (AS) in cloud droplets and aqueous aerosol particles. In this work, brown carbon formation in AS and other aerosol particles was quantified as a function of relative humidity (RH) during exposure to gas-phase glyoxal (GX) in chamber experiments. Under dry conditions (RH < 5%), solid AS, AS/glycine, and methylammonium sulfate aerosol particles brown within minutes upon exposure to GX, while sodium sulfate particles do not. When GX concentrations decline, browning goes away, demonstrating that this dry browning process is reversible. Declines in aerosol albedo are found to be a function of $[GX]^2$, and are consistent between AS and AS/glycine aerosol. Dry methylammonium sulfate aerosol browns 4× more than dry AS aerosol, but deliquesced AS aerosol browns much less than dry AS aerosol. Optical measurements at 405, 450, and 530 nm provide an estimated Ångstrom absorbance coefficient of -16 ±4. This coefficient and the empirical relationship between GX and albedo are used to estimate an upper limit to global radiative forcing by brown carbon formed by 70 ppt GX reacting with AS ($+7.6 \times 10^{-5}$ W/m^2). This quantity is < 1% of the total radiative forcing by secondary brown carbon, but occurs almost entirely in the ultraviolet range.

1 Introduction

Brown carbon is the name given to light-absorbing organic molecules present in atmospheric aerosol. Estimates of the global direct radiative effect of brown carbon aerosol range from +0.05 to 0.27 W/m^2 (Tuccella et al., 2020;Laskin et al., 2015;Zhang et al., 2019;Wang et al., 2018). This absorption occurs mainly at ultraviolet (UV) and near-UV wavelengths, suppressing photochemistry in areas with high loadings (Mok et al., 2016). Limiting emissions of brown carbon aerosol and its precursor species could provide immediate climate benefits. Approximately 30% of brown carbon is secondary (Mukai and Ambe,

Deleted: (Mok et al., 2016)

1986;Hecobian et al., 2010), formed from gas-phase species often through reactions taking place in clouds, fog, and aqueous aerosol particles (Hecobian et al., 2010). Reactions between small, multi-function aldehydes such as glyoxal and ammonium salts (Shapiro et al., 2009;Kampf et al., 2012), and oxidation reactions of phenolic species (Chang and Thompson, 2010) are two examples of aqueous-phase brown carbon formation processes.

Glyoxal uptake to deliquesced ammonium sulfate particles is rapid (Kroll et al., 2005), but is difficult to detect on dry aerosol (Corrigan et al., 2008). Glyoxal reacts to form brown carbon imidazole derivatives in solutions containing ammonium ions (Shapiro et al., 2009;Noziere et al., 2009;Galloway et al., 2009;Yu et al., 2011;Kampf et al., 2012;Maxut et al., 2015) or primary amine species such as glycine or methylamine (De Haan et al., 2009a;De Haan et al., 2009b). While in bulk aqueous solution these reactions take hours to days (Shapiro et al., 2009;Noziere et al., 2009;Powelson et al., 2014), they can occur in minutes in aqueous aerosol particles, likely due to surface reactivity of glyoxal in its monohydrate form (De Haan et al., 2009a).

In this work, we report rapid and reversible browning of dry ammonium sulfate (AS), AS/glycine, and methylammonium sulfate (MeAS) aerosol particles upon exposure to gas phase glyoxal. This browning process is not accompanied by appreciable particle growth, and is reversed upon addition of water vapor.

2 Methods

2.1 Large chamber experiments

CESAM is a 4.2 m^3 temperature- and pressure-controlled, stirred, stainless steel chamber (Wang et al., 2011) with solar simulator lamps (Harris et al., 2017), held just above ambient pressure with automated flows of high purity O_2 and liquid N_2 boil-off at a respective 20/80 v/v ratio. The chamber gas phase contents were monitored by a relative humidity (RH) sensor (Vaisala HMP234 Humicap), long-path FTIR spectroscopy (Bruker Tensor 37, 182.5 ±0.5 m path length (Wang et al., 2011), glyoxal integrated 2950-2700 cm^{-1} band intensity = 6.34×10^{-18} cm $molec^{-1}$ (Eurochamp, 2010)), and high-resolution proton transfer reaction mass spectrometry (PTR-MS, KORE Tech. Series II, inlet temperature 100°C, proton transfer reactor P = 1.64 mbar, glow discharge P = 1.94 mbar, PTR entry voltage = 400 V, E/N ratio = 130). Polydisperse seed particles (TSI 3076 atomizer) were diffusion dried before addition to the dry chamber, then continuously sampled through a 1 m Nafion drying tube to scanning mobility particle sizing (SMPS, TSI, 20 – 900 nm) and cavity-attenuated phase shift single-scattering albedo (450 nm CAPS-ssa, Aerodyne) (Onasch et al., 2015) spectrometers. A particle-into-liquid sampler (PILS, Brechtel Manufacturing) sampled N_2-diluted chamber aerosol through an activated carbon denuder, into a capillary waveguide UV/vis spectrometer (LWCC-100, 0.94m pathlength). Water vapor was added in bursts from a stainless steel boiler (Wang et al., 2011), and chamber RH was subsequently stabilized by routing inlet N_2 flow through a heated high-purity water bubbler. A droplet spectrometer (Palas Welas Digital 2000, 0.5 to 15 μm diam., on chamber flange) (Wang et al., 2011) extended the size

range of detected aerosol into supermicron particles. CAPS-ssa aerosol extinction and scattering signals were zeroed against filtered chamber air every 5 min to ensure that any gas-phase species absorbing light at 450 nm does not influence measurements, and averaged to SMPS scan frequency. SMPS number and concentrations and PTR-MS signals were corrected for dilution caused by flows into the chamber. SMPS size distributions were also corrected using size-dependent wall losses measured for AS particles in the chamber.

2.2 Small chamber experiments

Additional experiments were conducted in a 300 L collapsible Tedlar chamber. Aerosols were generated from 0.1% w/w aqueous solutions (TSI 3076 atomizer) and diffusion dried (except in experiments on "wet" aerosol). Glyoxal production was monitored at the inlet by absorbance at 405 nm using a cavity ringdown (CRD) spectrometer and a cross section of 4.491×10^{-20} cm^2 molecule^{-1} (Volkamer et al., 2005b). Glyoxal concentrations at the chamber outlet were measured in test experiments to determine wall loss rates (~6.7×10^{-4} s^{-1}). Glyoxal inlet concentrations, flow mixing ratios, and wall loss rates were then used to estimate glyoxal chamber concentrations. Aerosol particles were sampled via diffusion driers by Q-AMS (Aerodyne), CAPS-ssa (Aerodyne, 450 nm), SMPS (TSI), CRD (405 and 530 nm) (Ugelow et al., 2017), and photoacoustic spectrometers (PAS, 405 and 530 nm) (Ugelow et al., 2017), all of which were periodically baselined through filters to eliminate interferences by gas-phase species. RH sensors monitored humidity levels at the aerosol inlet, chamber outlet, and dried chamber outlet flows. Water vapor was added in certain experiments by passing inlet flows through Nafion humidifiers.

2.3 Chemicals

Reagents were used as received from Sigma-Aldrich unless otherwise mentioned. Solutions for aerosol generation were generated by dilution of glycine (>99%) to 5 mM, AS (>99%) to 1.2 – 10 mM, or sodium sulfate (≥99%) to 7 mM in deionized water (>18 MΩ, ELGA Maxima). MeAS was generated by mixing methylamine and sulfuric acid (Mallinckrodt) solutions at a 2:1 molar ratio; after dilution to 6.3 mM, solution pH was 4.5. Gas-phase glyoxal was generated by heating solid mixtures of glyoxal trimer dihydrate (Fluka, >95%) and P_2O_5 (99%) to 110-150 °C; the glyoxal produced was flushed into the chamber with dry N_2 (Volkamer et al., 2009).

3. Results

Chamber experiments where aerosol particles were exposed to gas-phase glyoxal are summarized in Table 1.

3.1 Dry AS and AS/glycine aerosol (experiments 1-4)

Experiment 1, where dry AS aerosol was sequentially exposed to 0.05 ppm and then 0.50 ppm glyoxal at t = 4:47 and 5:16 h, respectively, is summarized in Figure 1. Both glyoxal additions were detectable by PTR-MS at m/z 31 and 59. The m/z 59 signal, however, is elevated in the clean and dry chamber before glyoxal is added, indicating background interference by

Deleted: do

Deleted: for

Deleted: Aerosol particles were sampled via diffusion driers by Q-AMS (Aerodyne), CAPS-ssa (Aerodyne, 450 nm), SMPS (TSI), CRD (530 nm) (Ugelow et al., 2017)

Deleted: (Ugelow et al., 2017).

Deleted: (

another chemical species or its fragment in the mass spectrometer. SMPS data, which has been corrected for wall losses and for dilution, shows no observable aerosol growth after either glyoxal gas addition. This lack of observed growth at <5% RH is consistent with previous studies under very dry conditions (Kroll et al., 2005;De Haan et al., 2017). However, as optical and chemical measurements described below will show, this lack of growth does not indicate a lack of glyoxal reactivity.

The addition of 0.05 ppm glyoxal gas at t = 4:47 h triggered a short-lived drop in albedo by 0.034 that was observed by CAPS-ssa at 450 nm. A second, larger glyoxal addition (0.50 ppm) at t = 5:16 h caused albedo to plummet to 0.75, a change 7× greater than the first. Even though particle sizes did not increase after either glyoxal addition, the significant albedo declines indicate that glyoxal reactions rapidly produced light-absorbing products at dry AS particle surfaces. Over the next 30 minutes, as glyoxal gas-phase concentrations decreased by half (likely to due to chamber wall losses), aerosol albedo recovered proportionately, indicating that this surface brown carbon formation under dry conditions is fully reversible.

At t = 5:46 h (Figure 1), the chamber was humidified to 50% RH, a level which would not deliquesce the AS seeds (Biskos et al., 2006) but which may produce as many as 1-2 monolayers of adsorbed water at aerosol surfaces consisting of solid AS (Denjean et al., 2014;Romakkaniemi et al., 2001) or glyoxal reaction products. (Hawkins et al., 2014). Humidification to 50% RH caused significant changes to both the gas and aerosol phases. Glyoxal PTR-MS signals and aerosol albedo returned within a few minutes back to near-baseline levels, while the dried aerosol mass measured by SMPS jumped downward by 15%. The loss of gas-phase glyoxal, again without aerosol growth, suggests that water greatly accelerated glyoxal loss rates to the steel chamber walls. The simultaneous albedo recovery and SMPS mass loss indicate that humidification destroyed all brown carbon products that absorb 450 nm light, converting some fraction of them to gas-phase products. A proposed mechanism for this process is discussed below. It is significant that no browning was observed in PILS-sampled aerosol at any point during experiment 1, presumably due to the same mechanism occurring during wet sampling.

The 15% aerosol mass loss upon humidification to 50% RH is surprising, given that no corresponding mass gain was recorded during exposure to glyoxal under dry conditions. However, the lack of mass gain under dry conditions cannot be interpreted as a lack of glyoxal uptake or reactivity, given the large observed drop in albedo. Instead, the mass loss upon humidification suggests that at least 15% of the volume of AS seeds had been replaced under dry conditions by glyoxal reaction products that could break down into gas phase species once water was added. Simultaneous increases in gas-phase PTR-MS signals for m/z 47 (formic acid) and 61 (acetic acid) indicate that these acids were two of the gas-phase products generated by humidification. Formic acid is a known byproduct of imidazole production by aqueous-phase glyoxal + ammonia reactions (De Haan et al., 2009a;Yu et al., 2011).

Dried seed aerosol particles atomized from AS-glycine mixtures were also exposed to 0.25 ppm glyoxal under dry conditions in experiment 2 (Figure S1). The response of these internally mixed seeds to glyoxal exposure was comparable to that of pure

Deleted: .)

Deleted: is not surprising since the glyoxal additions occurred

Deleted: , and

Deleted: the lack up uptake of α-dicarbonyl compounds observed in

Deleted: caused detectable increases in PTR-MS signals at m/z 31 and 59. At the same time,

Deleted: produced much

Deleted: increases in gas-phase

Deleted: PTR-MS signals, and a sudden albedo decrease to 0.75.

Deleted: . Since SMPS data shows that particles were not detectably growing during this time (rather, aerosol mass declined by 5%), this loss of gas-phase glyoxal must have been largely to the steel

Deleted: walls. However, the large albedo decline without particle growth indicates that at least some glyoxal is causing browning reactions at dry particle surfaces. As gas-phase glyoxal concentrations declined,

Deleted: When

Deleted: cause measurable water uptake by AS (Denjean et al., 2014) or glyoxal reaction products

Deleted: ,

Deleted: were observed in

Deleted: (at t = 5:46 in Figure 1).

Deleted: suggest

Deleted: destroys the light-absorbing

Deleted: of the "dry browning" process residing at the solid aerosol surface

Deleted: (

Deleted: in

Deleted: destruction

Deleted: "

Deleted: browning"

Deleted: by water during sampling.)

Deleted: are

AS seeds. No growth was observed by SMPS, and aerosol albedo at 450 nm was anticorrelated with PTR-MS glyoxal signals at *m/z* 59, as before. The most significant difference between the experiments is that there was no 15% loss of aerosol mass observed by SMPS upon humidification of the chamber to 50% RH, even though acetic and formic acid were again released into the gas phase. This may be due to the lower volatility of deprotonated seed particle materials (glycine vs. ammonia). In addition, most glycine-derivatized imidazole products have permanent positive charges and are not in equilibrium with volatile neutral forms (De Haan et al., 2009a).

To better understand the reactive processes happening in the dry aerosol particles, further experiments were conducted in a 300 L Tedlar chamber probed by Q-AMS, SMPS, CAPS-ssa, and CRD/PAS. Figure S2 shows an AMS ion correlation plot comparing average signals before and after 40 ppb glyoxal was added over a period of 25 minutes to the dry chamber containing AS aerosol in experiment 3. Unsurprisingly, the slow addition of this smaller amount of glyoxal did not cause observable net particle growth or a decline in aerosol albedo at 450 nm. A marginal (0.9 μg/m^3, S/N = 1.6) increase in total organic aerosol was observed by Q-AMS during glyoxal addition, associated with significant increases (+30% or more relative to conserved aerosol species) in ion signals at *m/z* 15 (CH_3^+ or NH^+ fragments), 23 (Na^+), 29 (CHO^+ fragment), 47 (formic acid+H^+ or a $CH_3O_2^+$ fragment), 69 (imidazole-H^+), 81 (pyrazine-H^+), 97 and 119 (imidazole carboxyaldehyde "IC" +H^+ and Na^+, respectively). Slight decreases in aerosol water signals were observed at *m/z* 16. The detection of particle-phase imidazole, pyrazine, and IC suggests the presence of larger, light-absorbing molecules such as 2,2'-biimidazole and N-heterocycle derivatives that are typically associated with the products detected here (Kampf et al., 2012;Hawkins et al., 2018;Grace et al., 2019). However, detection of the larger product molecules directly from dry aerosol may require a soft, direct ionization technique such as extractive electrospray ionization (EESI-) MS.

Proposed chemical mechanisms for brown carbon production at AS particle surfaces are summarized in Schemes 1 and S1. Except for steps where new N-heterocyclic rings are formed, all processes are reversible (Kampf et al., 2012). Thus, a reduction of gas-phase glyoxal concentrations will shift reversible reactions away from BrC back towards simple N-heterocycle products, which do not absorb 450 nm light. Humidification to 50% RH accelerates this shift by removing more glyoxal from the gas phase, and perhaps also by hydrolysis of double bonds and dilution effects (Rincón et al., 2010;Phillips and Smith, 2014, 2015). Humidification also triggers the observed evaporation of formate as formic acid, and perhaps the evaporation of other small N-containing products.

The anticorrelation of albedo with glyoxal concentrations in experiments 1-4 is summarized in Figure 2. Although AS-glycine-glyoxal bulk aqueous mixtures have been shown to brown more than mixtures without glycine (Trainic et al., 2012;Powelson et al., 2014), here we see that dry AS and AS/glycine aerosol particles brown similarly for a given concentration of gas-phase glyoxal. This may indicate that glycine is not at the aerosol surface, or that glycine surfaces, when present, are less able to

Deleted: The
Deleted: an
Deleted: , but increases
Deleted: -phase ion signals were
Deleted: multiple experiments
Deleted: and 69 (protonated imidazole), while slight decreases in aerosol water signals were observed at *m/z* 16. Increases were seen in single experiments at *m/z*
Deleted: +
Deleted:).)
Deleted: presence
Deleted:
Deleted: formic acid
Deleted: that
Deleted: (Kampf et al., 2012) may also be present.
Deleted: these

retain adsorbed water in the dry chamber. We therefore fit the combined dataset from all 4 experiments. Albedo shows a clear downward curvature at high glyoxal concentrations, such that the relationship is best fit by a 2nd order polynomial. This suggests that the formation of the compounds absorbing at 450 nm is proportional to [glyoxal]^2. While glyoxal + ammonium reactions are 1st order in glyoxal in dilute solution when [glyoxal] × [NH_4^+] < 1.2 M, they switch to 2nd order at higher concentrations (Noziere et al., 2009), which are likely in these dry experiments.

Reversible surface browning of AS aerosol under dry conditions was also recently observed during exposures to methylglyoxal gas (De Haan et al., 2017). The albedo values observed before and after two methylglyoxal additions are shown for comparison in Figure 2. Although the data shows a slight negative offset due to particle size effects, judging by the slope it is clear that methylglyoxal's effect on the albedo of dry AS aerosol is significantly less than glyoxal. This is the opposite of the trend in brown carbon production in bulk aqueous solutions at pH 5, where methylglyoxal is much more effective in generating light-absorbing products (Powelson et al., 2014), perhaps due to the fact that its ketone functional group is far less likely to be inactivated by hydration than the aldehyde groups on both molecules. However, in these dry aerosol experiments where water is scarce, glyoxal's greater attraction to water (seen in its much higher Henry's law coefficient) (Betterton and Hoffmann, 1988;Ip et al., 2009;Kampf et al., 2013) may allow it to interact with small amounts of adsorbed water at the AS aerosol surface far more effectively than methylglyoxal.

3.2 Dry MeAS or sodium sulfate aerosol (experiments 5 - 6)

Deleted: 8 - 9

Gas phase glyoxal was added to a few other types of seed particles in the small chamber. In experiments on MeAS seeds (expt. 5, Figure 3 top panel), the slow addition of 140 ppb of glyoxal caused a matching drop of -0.15 in aerosol albedo measured by CAPS-ssa at 450 nm and an increase in aerosol absorbance to 28 Mm^{-1} measured by PAS at 405 nm. The albedo decline at 450 nm (Figure 2, green circles) is 4× greater than observed on AS seeds at similar glyoxal concentrations. This result is consistent with earlier aqueous-phase studies showing greater browning in glyoxal – methylamine mixtures than in glyoxal – AS mixtures at the same pH (Powelson et al., 2014).

Deleted: 8

Albedo at 405 nm was calculated from PAS and CRD signals in expt. 5 (Figure S3), showing that albedo had dropped to 0.30 by 1:11 pm and remained at this level for 45 minutes. These albedo values indicate that maximum light absorbance at 405 nm was 4.7× greater than at 450 nm, and persisted for a longer period of time after glyoxal gas concentrations decline. At even longer wavelengths (530 nm), PAS aerosol absorbance reached only 0.9 Mm^{-1}, further indicating highly wavelength-dependent light absorption. The absorption spectra of atmospheric brown carbon are typically well-fit by exponential decay functions. Such featureless spectra can be characterized by an Ångstrom absorption coefficient α, which is the slope of a log(absorbance) vs log(wavelength) plot. Comparing the amount of light absorbance at 405, 450, and 530 nm at 1:11 pm in experiment 5 gives α = -12.7 ±0.8 (Figure S5). A similar analysis of expt. 4 (Figures S6 and S7, dry AS + glyoxal), the only other experiment

Deleted: 8

Deleted: 8

with measurable absorbance at all 3 wavelengths, gives a comparable α = -16 ±4. Thus, it appears that brown carbon formed by glyoxal under dry conditions on AS and MeAS aerosol absorb light with similar wavelength dependence.

In an experiment on dry sodium sulfate seeds at ~35% RH in the small Tedlar chamber (expt. 6, Figure 3) glyoxal concentrations were increased from zero to ~2000 ppb over 30 min. During this time, albedo at 450 nm remained at 1 ±0.005, and no aerosol absorbance was measured by PAS at either 530 or 405 nm. The lack of browning observed even at such high glyoxal concentrations confirms that ammonium or methylammonium ions (or ammonia or methylamine) are necessary reaction partners with glyoxal in the browning process observed in experiments 1-5. It also confirms that our CAPS and PAS measurements are not biased by absorbance due to gas-phase glyoxal.

3.3 Deliquesced AS aerosol (experiments 7-9)

Finally, three experiments exploring browning on wet rather than dry AS aerosol were conducted at RH ranging from 38 to 81%. The highest humidity experiment (expt. 7) is summarized in Figure S8. In experiments 7–9, albedo declines of 0.013 or less were observed following addition of 1.1, 1.2, and 0.12 ppm of glyoxal gas, respectively. If graphed in Figure 2, the resulting slopes for experiments 7-8 would be more than 1000x flatter than the methylglyoxal data shown for comparison. While some of the glyoxal gas added may have been quickly lost to the walls of the humid chambers as an equilibrium is established (Kroll et al., 2005), especially in experiments 7 and 9, it is clear that wet AS aerosol particles brown much less than dry AS, AS/glycine, or MeAS aerosol upon exposure to glyoxal.

Enhanced AS aerosol browning under dry conditions is surprising, given that glyoxal Maillard chemistry is normally considered an aqueous-phase process. One clue to the nature of the dry browning process is seen in the slight depletion of water signals observed in all dry experiments probed by Q-AMS (#3, 4, 5, Figures S2 and S9) after browning caused by glyoxal exposure. (Most water is removed from aerosol particles in the AMS inlet.) The extra water depletion associated with glyoxal exposure of dry aerosol, which was not observed in deliquesced aerosol experiments probed by Q-AMS (#7-8), suggests that even under dry conditions, glyoxal is able to access and deplete trace amounts of aerosol-phase surface water. Any adsorbed water would be saturated with ammonium (or methylammonium) sulfate, and the presence of dissolved AS is known to greatly increase glyoxal uptake via a "salting in" effect (Kampf et al., 2013;Waxman et al., 2015), while methylglyoxal solubility is reduced by salting out (Waxman et al., 2015). Thus, both glyoxal and AS are expected to be concentrated in any surface-adsorbed water present. In a previous study, similar reasoning was used to explain glyoxal uptake on solid seed particles at RH levels as low as 10% (Corrigan et al., 2008). Furthermore, the scarcity of water will favor dehydration of products, helping to form light-absorbing conjugated double bonds.

Deleted: 9

Deleted: 4 and 8

Deleted: 5-

Deleted: the three

Deleted: 0.12,

Deleted: 1.2

Deleted: 6-

Deleted: 5-6

Deleted: 8

Deleted: S8

Deleted: 6-

4 Discussion

Since methylglyoxal is generally less abundant in the atmosphere than glyoxal (Igawa et al., 1989;Munger et al., 1995;Matsumoto et al., 2005), and since the browning of dry AS by methylglyoxal is much less than that of glyoxal likely due to salting effects (Kampf et al., 2013;Waxman et al., 2015), we will focus on the effects of instantaneous browning of atmospheric aerosol particles due to interaction with glyoxal. We will assume that all tropospheric sulfate particles contain ammonium, and, as an upper limit, that solid-phase tropospheric sulfate particles would brown as much as the pure, fully dry AS particles used in this study regardless of the presence of additional aerosol species. The first assumption is generally reasonable (Jimenez et al., 2009), since acidic sulfate aerosol takes up ammonia in the atmosphere, while the second assumption will clearly result in the estimation of an upper limit, since the presence of other materials at aerosol particle surfaces has been shown to limit the extent of the interactions between glyoxal and ammonium ions (Drozd and McNeill, 2014), and few locations in the troposphere are as dry as in this study. Tropospheric aerosol particles are typically semi-solid or solid phase, except low over the Amazon and Arctic (Shiraiwa et al., 2017).

Using the function $albedo = -0.97[GX]^2 - 0.16[GX] + 1.00$ from Figure 2, a global 24-h average glyoxal concentration of ~70 ppt (Fu et al., 2008;Zhou and Mopper, 1990;Munger et al., 1995;Spaulding et al., 2003;Matsunaga et al., 2004;Müller et al., 2005;Ieda et al., 2006) would lower particle albedo at 450 nm ($\Delta Albedo(450)$) by only 1.1×10^{-5}. Using our measured Ångstrom absorption coefficient $\alpha = -16$ for glyoxal + AS brown carbon formed under dry conditions, we estimated albedo depression at other wavelengths ($\Delta Albedo(\lambda)$) between 280 and 4000 nm using Eq. (1):

$$\frac{\log\left(\frac{\Delta Albedo(\lambda)}{\Delta Albedo(450)}\right)}{\log\left(\frac{\lambda}{450}\right)} = \alpha \quad (1)$$

These albedo decreases were multiplied by the solar spectrum (ASTM G173-03) times the wavelength-dependent scattering function of AS aerosol (Nemesure et al., 1995) at each wavelength (Figure S10), and then integrated across the spectrum. 97% of the solar energy absorbed by this brown carbon source is predicted to be in the UV range, with the absorbed energy peaking near 330 nm. The total fraction of energy absorbed by glyoxal + AS brown carbon (absorption × solar spectrum × scattering function) is calculated to be 1.9×10^{-4}, relative to the total energy scattered by AS aerosol (solar spectrum × scattering function). We then multiply this energy fraction times the magnitude of global direct radiative forcing due to sulfate scattering, estimated by the IPCC to be -0.4 ±0.2 W/m^2 (Ramaswamy et al., 2018), to quantify a global radiative forcing of $+7.6 \times 10^{-5}$ W/m^2 by dry browning of ammonium sulfate aerosol. This climate forcing is negligible compared to the global net aerosol direct effect (-0.45 ±0.5 W/m^2) or absorption by black carbon ($+0.4\ ^{+0.4}_{-0.35}$ W/m^2) (Ramaswamy et al., 2018), and is less than 1% of estimates of radiative forcing by secondary brown carbon (+0.015 to +0.081 W/m^2) (Mukai and Ambe, 1986;Hecobian et al.,

Deleted: . While
Deleted: , tropospheric
Deleted: is nevertheless
Formatted: Font: Italic
Formatted: Font: Italic
Deleted: function
Deleted: 1990b;Zhou and Mopper, 1990a
Deleted: S9
Deleted: (Ramaswamy et al., 2018)
Deleted: (Ramaswamy et al., 2018)

2010;Shamjad et al., 2015;Tuccella et al., 2020). While dry browning of ammonium sulfate aerosol in the presence of ambient glyoxal thus does not appear to be globally significant in terms of radiative forcing, it may be regionally significant in polluted areas where glyoxal concentrations can greatly exceed 70 ppt (Volkamer et al., 2005a), where larger loadings of AS aerosol are present, or where aerosol browning by glyoxal occurs in the upper troposphere (Zhang et al., 2017).

5 Supporting Information

Supporting Information is available: proposed reaction scheme including humidification, data summaries of experiments 2, 4, 7, 8, and 9, Ångstrom coefficient plots for experiments 4 and 8, Q-AMS plots summarizing the effects of glyoxal addition in experiments 3 and 8, and estimated spectrum of absorbance of sulfate-scattered solar radiation due to glyoxal uptake.

6 Acknowledgments

This work was funded by NSF grant AGS-1523178 and AGS-1826593. L. N. Hawkins was funded by the Barbara Stokes Dewey Foundation and Research Corporation (CCSA 22473). The authors thank Mila Ródenas García (CEAM) for access to the *Main Polwin* MATLAB program and for glyoxal FTIR reference spectra. CNRS-INSU is gratefully acknowledged for supporting CESAM as an open facility through the National Instrument label. The CESAM chamber has received funding from the European Union's Horizon 2020 research and innovation program through the EUROCHAMP-2020 Infrastructure Activity under grant agreement No 730997.

Data availability

Data is available from the authors upon request.

Author Contributions

David De Haan guided the project and wrote the manuscript. Lelia Hawkins and Jean-François Doussin guided large chamber experiments. Margaret Tolbert guided small chamber experiments. Kevin Jansen conducted small chamber experiments. Hannah Welsh, Raunak Pednekar, Alexia de Loera, Natalie Jimenez, Mathieu Cazaunau, and Edouard Pangui conducted large chamber experiments. Aline Gratien and Antonin Bergé quantified glyoxal by FTIR in the large chamber. Paola Formenti provided assistance in interpreting optical measurements.

Competing Interests

The authors declare no competing interests.

References

Betterton, E. A., and Hoffmann, M. R.: Henry's Law constants of some environmentally important aldehydes, Environ. Sci. Technol., 22, 1415-1418, 10.1021/es00177a004, 1988.

Biskos, G., Paulsen, D., Russell, L. M., Buseck, P. R., and Martin, S. T.: Prompt deliquescence and efflorescence of aerosol nanoparticles, Atmos. Chem. Phys., 6, 4633-4642, 10.5194/acp-6-4633-2006, 2006.

Chang, J. L., and Thompson, J. E.: Characterization of colored products formed during irradiation of solutions containing H_2O_2 and phenolic compounds, Atmos. Environ., 44, 541-551, 10.1016/j.atmosenv.2009.10.042, 2010.

Clegg, S. L., and Wexler, A. S.: Densities and Apparent Molar Volumes of Atmospherically Important Electrolyte Solutions. 1. The Solutes H2SO4, HNO3, HCl, Na2SO4, NaNO3, NaCl, (NH4)2SO4, NH4NO3, and NH4Cl from 0 to 50 °C, Including Extrapolations to Very Low Temperature and to the Pure Liquid State, and NaHSO4, NaOH, and NH3 at 25 °C, The Journal of Physical Chemistry A, 115, 3393-3460, 10.1021/jp108992a, 2011.

Corrigan, A. L., Hanley, S. W., and De Haan, D. O.: Uptake of glyoxal by organic and inorganic aerosol, Environ. Sci. Technol., 42, 4428-4433, 10.1021/es7032394, 2008.

De Haan, D. O., Corrigan, A. L., Smith, K. W., Stroik, D. R., Turley, J. T., Lee, F. E., Tolbert, M. A., Jimenez, J. L., Cordova, K. E., and Ferrell, G. R.: Secondary organic aerosol-forming reactions of glyoxal with amino acids, Environ. Sci. Technol., 43, 2818-2824, 10.1021/es803534f, 2009a.

De Haan, D. O., Tolbert, M. A., and Jimenez, J. L.: Atmospheric condensed-phase reactions of glyoxal with methylamine, Geophys. Res. Lett., 36, L11819, 10.1029/2009GL037441, 2009b.

De Haan, D. O., Hawkins, L. N., Welsh, H. G., Pednekar, R., Casar, J. R., Pennington, E. A., de Loera, A., Jimenez, N. G., Symons, M. A., Zauscher, M., Pajunoja, A., Caponi, L., Cazaunau, M., Formenti, P., Gratien, A., Pangui, E., and Doussin, J. F.: Brown carbon production in ammonium- or amine-containing aerosol particles by reactive uptake of methylglyoxal and photolytic cloud cycling, Environ Sci Technol, 51, 7458-7466, 10.1021/acs.est.7b00159, 2017.

Denjean, C., Formenti, P., Picquet-Varrault, B., Katrib, Y., Pangui, E., Zapf, P., and Doussin, J. F.: A new experimental approach to study the hygroscopic and optical properties of aerosols: application to ammonium sulfate particles, Atmos. Meas. Tech., 7, 183-197, 10.5194/amt-7-183-2014, 2014.

Drozd, G. T., and McNeill, V. F.: Organic matrix effects on the formation of light-absorbing compounds from [small alpha]-dicarbonyls in aqueous salt solution, Environmental Science: Processes & Impacts, 16, 741-747, 10.1039/C3EM00579H, 2014.

Fu, T.-M., Jacob, D. J., Wittrock, F., Burrows, J. P., Vrekoussis, M., and Henze, D. K.: Global budgets of atmospheric glyoxal and methylglyoxal, and implications for formation of secondary organic aerosols, J. Geophys. Res., 113, D15303, 10.1029/2007JD009505, 2008.

Galloway, M. M., Chhabra, P. S., Chan, A. W. H., Surratt, J. D., Flagan, R. C., Seinfeld, J. H., and Keutsch, F. N.: Glyoxal uptake on ammonium sulphate seed aerosol: reaction products and reversibility of uptake under dark and irradiated conditions, Atmos. Chem. Phys., 9, 3331-3345, 10.5194/acp-9-3331-2009, 2009.

Grace, D. N., Sharp, J. R., Holappa, R. E., Lugos, E. N., Sebold, M. B., Griffith, D. R., Hendrickson, H. P., and Galloway, M. M.: Heterocyclic Product Formation in Aqueous Brown Carbon Systems, ACS Earth and Space Chemistry, 3, 2472-2481, 10.1021/acsearthspacechem.9b00235, 2019.

Harris, A., Cazaunau, M., Gratien, A., Pangui, E., and Doussin, J.-F.: Atmospheric Simulation Chamber Studies of the Gas-Phase Photolysis of Pyruvic Acid, The Journal of Physical Chemistry A, 121, 10.1021/acs.jpca.7b05139, 2017.

Hawkins, L. N., Baril, M. J., Sedehi, N., Galloway, M. M., De Haan, D. O., Schill, G. P., and Tolbert, M. A.: Formation of semi-solid, oligomerized aqueous SOA: Lab simulations of cloud processing, Environ Sci Technol, 48, 2273-2280, 10.1021/es4049626, 2014.

Hawkins, L. N., Welsh, H. G., and Alexander, M. V.: Evidence for pyrazine-based chromophores in cloud water mimics containing methylglyoxal and ammonium sulfate, Atmos. Chem. Phys., 18, 12413-12431, 10.5194/acp-18-12413-2018, 2018.

Hecobian, A., Zhang, X., Zheng, M., Frank, N., Edgerton, E. S., and Weber, R. J.: Water-soluble organic aerosol material and the light-absorption characteristics of aqueous extracts measured over the southeastern United States., Atmos. Chem. Phys., 10, 5965-5977, 10.5194/acp-10-5965-2010, 2010.

Formatted: Space After: 0 pt

Formatted: Space After: 0 pt

Formatted: Space After: 0 pt

Formatted: Space After: 0 pt

Ieda, T., Kitamori, Y., Mochida, M., Hirata, R., Hirano, T., Inukai, K., Fujinuma, Y., and Kawamura, K.: Diurnal variations and vertical gradients of biogenic volatile and semi-volatile organic compounds at the Tomakomai larch forest station in Japan, Tellus B: Chemical and Physical Meteorology, 58, 177-186, 10.1111/j.1600-0889.2006.00179.x, 2006.

Igawa, M., Munger, J. W., and Hoffmann, M. R.: Analysis of aldehydes in cloud- and fogwater samples by HPLC with a postcolumn reaction detector, Environ. Sci. Technol., 23, 556-561, 10.1021/es00063a007, 1989.

Ip, H. S. S., Huang, X. H. H., and Yu, J. Z.: Effective Henry's law constants of glyoxal, glyoxylic acid, and glycolic acid, Geophys. Res. Lett., 36, L01802, 10.1029/2008gl036212, 2009.

Jimenez, J. L., Canagaratna, M. R., Donahue, N. M., Prevot, A. S. H., Zhang, Q., Kroll, J. H., DeCarlo, P. F., Allan, J. D., Coe, H., Ng, N. L., Aiken, A. C., Docherty, K. S., Ulbrich, I. M., Grieshop, A. P., Robinson, A. L., Duplissy, J., Smith, J. D., Wilson, K. R., Lanz, V. A., Hueglin, C., Sun, Y. L., Tian, J., Laadsonen, A., Raatikainen, T., Rautiainen, J., Vaattovaara, P., Ehn, M., Kulmala, M., Tomlinson, J. M., Collins, D. R., Cubison, M. J., Dunlea, E. J., Huffman, J. A., Onasch, T. B., Alfarra, M. R., Williams, P. I., Bower, K., Kondo, Y., Schneider, J., Drewnick, F., Borrmann, S., Weimer, S., Demerjian, K., Salcedo, D., Cottrell, L., Griffin, R., Takami, A., Miyoshi, T., Hatakeyama, S., Shimono, A., Sun, J. Y., Zhang, Y. M., Dzepina, K., Kimmel, J. R., Sueper, D., Jayne, J. T., Herndon, S. C., Trimborn, A. M., Williams, L. R., Wood, E. C., Middlebrook, A. M., Kolb, C. E., Baltensperger, U., and Worsnop, D. R.: Evolution of organic aerosols in the atmosphere, Science, 326, 1525-1529, 10.1126/science.1180353, 2009.

Kampf, C. J., Jakob, R., and Hoffmann, T.: Identification and characterization of aging products in the glyoxal/ammonium sulfate system -- implications for light-absorbing material in atmospheric aerosols, Atmos. Chem. Phys., 12, 6323-6333, 10.5194/acp-12-6323-2012, 2012.

Kampf, C. J., Waxman, E. M., Slowik, J. G., Dommen, J., Pfaffenberger, L., Praplan, A. P., Prévôt, A. S. H., Baltensperger, U., Hoffmann, T., and Volkamer, R.: Effective Henry's Law Partitioning and the Salting Constant of Glyoxal in Aerosols Containing Sulfate, Environ Sci Technol, 47, 4236-4244, 10.1021/es400083d, 2013.

Kroll, J. H., Ng, N. L., Murphy, S. M., Varutbangkul, V., Flagan, R. C., and Seinfeld, J. H.: Chamber studies of secondary organic aerosol growth by reactive uptake of simple carbonyl compounds, J. Geophys. Res., 110, D23207, 10.1029/2005jd006004, 2005.

Laskin, A., Laskin, J., and Nizkorodov, S. A.: Chemistry of Atmospheric Brown Carbon, Chem. Rev., 115, 4335-4382, 10.1021/cr5006167, 2015.

Matsumoto, K., Kawai, S., and Igawa, M.: Dominant factors controlling concentrations of aldehydes in rain, fog, dew water, and in the gas phase., Atmos. Environ., 39, 7321-7329, 10.1016/j.atmosenv.2005.09.009, 2005.

Matsunaga, S., Mochida, M., and Kawamura, K.: Variation on the atmospheric concentrations of biogenic carbonyl compounds and their removal processes in the northern forest at Moshiri, Hokkaido Island in Japan, J. Geophys. Res., 109, D04302, 10.1029/2003JD004100, 2004.

Maxut, A., Noziere, B., Fenet, B., and Mechakra, H.: Formation mechanisms and yields of small imidazoles from reactions of glyoxal with NH4+ in water at neutral pH, Phys. Chem. Chem. Phys., 17, 20416-20424, 10.1039/C5CP03113C, 2015.

Merck Index 10th ed., Merck Co., Inc., Rahway, New Jersey, 1983.

Mok, J., Krotkov, N. A., Arola, A., Torres, O., Jethva, H., Andrade, M., Labow, G., Eck, T. F., Li, Z., Dickerson, R. R., Stenchikov, G. L., Osipov, S., and Ren, X.: Impacts of brown carbon from biomass burning on surface UV and ozone photochemistry in the Amazon Basin, Sci Rep, 6, 36940, 10.1038/srep36940, 2016.

Mukai, H., and Ambe, Y.: Characterization of a humic acid-like brown substance in airborne particulate matter and tentative identification of its origin, Atmospheric Environment (1967), 20, 813-819, https://doi.org/10.1016/0004-6981(86)90265-9, 1986.

Müller, K., van Pinxteren, D., Plewka, A., Svrcina, B., Kramberger, H., Hofmann, D., Bächmann, K., and Herrmann, H.: Aerosol characterisation at the FEBUKO upwind station Goldlauter (II): Detailed organic chemical characterisation, Atmos. Environ., 39, 4219-4231, https://doi.org/10.1016/j.atmosenv.2005.02.008, 2005.

Munger, J. W., Jacob, D. J., Daube, B. C., Horowitz, L. W., Keene, W. C., and Heikes, B. G.: Formaldehyde, glyoxal, and methylglyoxal in air and cloudwater at a rural mountain site in central Virginia, J. Geophys. Res., 100, 9325-9333, 10.1029/95JD00508, 1995.

Nemesure, S., Wagener, R., and Schwartz, S. E.: Direct shortwave forcing of climate by the anthropogenic sulfate aerosol: Sensitivity to particle size, composition, and relative humidity, Journal of Geophysical Research: Atmospheres, 100, 26105-26116, 10.1029/95JD02897, 1995.

Deleted: . O. U

Formatted: Space After: 0 pt

Deleted: Scientific Reports

Noziere, B., Dziedzic, P., and Cordova, A.: Products and kinetics of the liquid-phase reaction of glyoxal catalyzed by ammonium ions (NH_4^+), J. Phys. Chem., 113, 231-237, 10.1021/jp8078293, 2009.

Onasch, T. B., Massoli, P., Kebabian, P. L., Hills, F. B., Bacon, F. W., and Freedman, A.: Single scattering albedo monitor for airborne particulates., Aerosol Sci. Technol., 49, 267-279, 10.1080/02786826.2015.1022248, 2015.

Phillips, S. M., and Smith, G. D.: Light absorption by charge transfer complexes in brown carbon aerosols, Environ. Sci. Technol. Lett., 1, 382-386, 10.1021/ez500263j, 2014.

Phillips, S. M., and Smith, G. D.: Further evidence for charge transfer complexes in brown carbon aerosols from excitation-emission matrix fluorescence spectroscopy, J. Phys. Chem., 119, 4545-4551, 10.1021/jp510709e, 2015.

Powelson, M. H., Espelien, B. M., Hawkins, L. N., Galloway, M. M., and De Haan, D. O.: Brown carbon formation by aqueous-phase aldehyde reactions with amines and ammonium sulfate, Environ Sci Technol, 48, 985-993, 10.1021/es4038325, 2014.

Qiu, C., and Zhang, R.: Physiochemical Properties of Alkylaminium Sulfates: Hygroscopicity, Thermostability, and Density, Environ Sci Technol, 46, 4474-4480, 10.1021/es3004377, 2012.

Ramaswamy, V., Collins, W., Haywood, J., Lean, J., Mahowald, N., Myhre, G., Naik, V., Shine, K. P., Soden, B., Stenchikov, G., and Storelvmo, T.: Radiative Forcing of Climate: The Historical Evolution of the Radiative Forcing Concept, the Forcing Agents and their Quantification, and Applications, Meteorological Monographs, 59, 14.11-14.101, 10.1175/AMSMONOGRAPHS-D-19-0001.1, 2018.

Rincón, A. G., Guzmán, M. I., Hoffmann, M. R., and Colussi, A. J.: Thermochromism of model organic aerosol matter, J. Phys. Chem. Lett., 1, 368-373, 10.1021/jz900186e 2010.

Romakkaniemi, S., Hämeri, K., Väkevä, M., and Laaksonen, A.: Adsorption of Water on 8−15 nm NaCl and (NH4)2SO4 Aerosols Measured Using an Ultrafine Tandem Differential Mobility Analyzer, The Journal of Physical Chemistry A, 105, 8183-8188, 10.1021/jp010647l, 2001.

Shamjad, P. M., Tripathi, S. N., Pathak, R., Hallquist, M., Arola, A., and Bergin, M. H.: Contribution of Brown Carbon to Direct Radiative Forcing over the Indo-Gangetic Plain, Environ Sci Technol, 49, 10474-10481, 10.1021/acs.est.5b03368, 2015.

Shapiro, E. L., Szprengiel, J., Sareen, N., Jen, C. N., Giordano, M. R., and McNeill, V. F.: Light-absorbing secondary organic material formed by glyoxal in aqueous aerosol mimics, Atmos. Chem. Phys., 9, 2289-2300, 10.5194/acp-9-2289-2009, 2009.

Shiraiwa, M., Li, Y., Tsimpidi, A. P., Karydis, V. A., Berkemeier, T., Pandis, S. N., Lelieveld, J., Koop, T., and Pöschl, U.: Global distribution of particle phase state in atmospheric secondary organic aerosols, Nature Communications, 8, 15002, 10.1038/ncomms15002, 2017.

Spaulding, R. S., Schade, G. W., Goldstein, A. H., and Charles, M. J.: Characterization of secondary atmospheric photooxidation products: evidence for biogenic and anthropogenic sources, Journal of Geophysical Research, [Atmospheres], 108, 4247, 10.1029/2002JD002478, 2003.

Trainic, M., Abo Riziq, A., Lavi, A., and Rudich, Y.: Role of interfacial water in the heterogeneous uptake of glyoxal by mixed glycine and ammonium sulfate aerosols, J. Phys. Chem., 116, 5948-5957, 10.1021/jp2104837, 2012.

Tuccella, P., Curci, G., Pitari, G., Lee, S., and Jo, D. S.: Direct radiative effect of absorbing aerosols: sensitivity to mixing state, brown carbon and soil dust refractive index and shape, Journal of Geophysical Research: Atmospheres, n/a, 10.1029/2019JD030967, 2020.

Ugelow, M. S., Zarzana, K. J., Day, D. A., Jimenez, J. L., and Tolbert, M. A.: The optical and chemical properties of discharge generated organic haze using in-situ real-time techniques, Icarus, 294, 1-13, https://doi.org/10.1016/j.icarus.2017.04.028, 2017.

Volkamer, R., Molina, L. T., Molina, M. J., Shirley, T., and Brune, W. H.: DOAS measurement of glyoxal as an indicator for fast VOC chemistry in urban air, Geophys. Res. Lett., 32, L08806, 10.1029/2005GL022616, 2005a.

Volkamer, R., Spietz, P., Burrows, J., and Platt, U.: High-resolution absorption cross-section of glyoxal in the UV–vis and IR spectral ranges, Journal of Photochemistry and Photobiology A: Chemistry, 172, 35-46, https://doi.org/10.1016/j.jphotochem.2004.11.011, 2005b.

Volkamer, R., Ziemann, P. J., and Molina, M. J.: Secondary organic aerosol formation from acetylene (C_2H_2): seed effect on SOA yields due to organic photochemistry in the aerosol aqueous phase, Atmos. Chem. Phys., 9, 1907-1928, 10.5194/acp-9-1907-2009, 2009.

Formatted: Space After: 0 pt

Formatted: Space After: 0 pt

Formatted: Space After: 0 pt

Wang, J., Doussin, J. F., Perrier, S., Perraudin, E., Katrib, Y., Pangui, E., and Picquet-Varrault, B.: Design of a new multi-phase experimental simulation chamber for atmospheric photosmog, aerosol and cloud chemistry research, Atmos. Meas. Tech., 4, 2465-2494, 10.5194/amt-4-2465-2011, 2011.

Wang, X., Heald, C. L., Liu, J., Weber, R. J., Campuzano-Jost, P., Jimenez, J. L., Schwarz, J. P., and Perring, A. E.: Exploring the observational constraints on the simulation of brown carbon, Atmos. Chem. Phys., 18, 635-653, 10.5194/acp-18-635-2018, 2018.

Waxman, E. M., Elm, J., Kurtén, T., Mikkelsen, K. V., Ziemann, P. J., and Volkamer, R.: Glyoxal and Methylglyoxal Setschenow Salting Constants in Sulfate, Nitrate, and Chloride Solutions: Measurements and Gibbs Energies, Environ Sci Technol, 49, 11500-11508, 10.1021/acs.est.5b02782, 2015.

Yu, G., Bayer, A. R., Galloway, M. M., Korshavn, K. J., Fry, C. G., and Keutsch, F. N.: Glyoxal in aqueous ammonium sulfate solutions: products, kinetics, and hydration effects, Environ. Sci. Technol., 45, 6336-6342, 10.1021/es200989n, 2011.

Zhang, A., Wang, Y., Zhang, Y., Weber, R. J., Song, Y., Ke, Z., and Zou, Y.: Modeling global radiative effect of brown carbon: A larger heating source in the tropical free troposphere than black carbon, Atmos. Chem. Phys. Discuss., 2019, 1-36, 10.5194/acp-2019-594, 2019.

Zhang, Y., Forrister, H., Liu, J., Dibb, J., Anderson, B., Schwarz, J. P., Perring, A. E., Jimenez, J. L., Campuzano-Jost, P., Wang, Y., Nenes, A., and Weber, R. J.: Top-of-atmosphere radiative forcing affected by brown carbon in the upper troposphere, Nature Geosci., 10, 486, 10.1038/ngeo2960, 2017.

Zhou, X., and Mopper, K.: Apparent partition coefficients of 15 carbonyl compounds between air and seawater and between air and freshwater; implications for air-sea exchange, Environ. Sci. Technol., 24, 1864-1869, 1990.

Deleted: Measurement

Deleted: sub-parts-per-billion levels of

Deleted: in marine

Deleted: by a simple cartridge trapping procedure followed by liquid chromatography

Formatted: Space After: 10 pt

Deleted: ,

Deleted: 1482-1485, 10.1021/es00080a004, 1990a

Deleted: Zhou, X., and Mopper, K.: Apparent partition coefficients of 15 carbonyl compounds between air and seawater and between air and freshwater; implications for air-sea exchange, Environ. Sci. Technol., 24, 1864-1869, 1990b.¶

Formatted: Space After: 0 pt, Line spacing: 1.5 lines

Deleted: ¶
¶

Formatted: Font: Not Bold

Table 1: Summary of Glyoxal Gas Addition Experiments:

Expt #	[GX][a] (ppm)	aerosol type	seed aerosol conc. ($\mu g/m^3$)	seed density (g/cm^3)	RH at glyoxal addition (%)	mass increase ($\mu g/m^3$)	albedo change, 450 nm
1a	0.05	AS	145	1.77	< 5	< 0.3	-0.034[b]
1b	0.50	AS	145	1.77	< 5	-3 (decr)	-0.233[b]
2	0.25	AS/Gly	100	1.30	< 5	< 1	-0.094[b]
3[c]	0.04[d]	AS	90	1.77	< 5	0.9[e,f]	-0.001
4[c]	0.30[d]	AS	40[f]	1.77	< 5	< 1	-0.069
5[c]	0.14[d]	MeAS	80[f]	1.44[g]	< 5	< 1	-0.15
6[c]	2.0[d]	Na_2SO_4	70[f]	1.46[h]	35	< 1	0
7[c]	1.1[d]	wet AS	180[f]	1.24[i]	81	< 1	-0.012
8[c]	~1.2[d]	wet AS	170	1.43[i]	38	< 1	-0.010
9	0.12[j]	wet AS	90	1.26[i]	77	< 1.6	-0.013[b]

Notes: GX = glyoxal; AS = ammonium sulfate; Gly = glycine; MeAS = methylammonium sulfate. **a**: Tabulated GX concentrations are peak values measured by PTR-MS, ±20% rel. uncertainty unless otherwise stated. **b**: occurring within 5 min. of GX pulse addition. **c**: Experiment performed in 300 L Tedlar bag. **d**: GX added gradually rather than in pulse; max. concentration estimated from PAS measurements at chamber inlet. **e**: Organic aerosol growth. **f**: measured by Q-AMS. **g**: from (Qiu and Zhang, 2012). **h**: from (Merck, 1983), for the decahydrate. **i**: from AIM model IV (Clegg and Wexler, 2011) **j**: Estimated from addition bulb pressure and comparison of PTR-MS signals of *m/z* 72 imine product.

Formatted ... [5]
Formatted ... [1]
Inserted Cells ... [7]
Formatted ... [3]
Formatted Table ... [2]
Formatted ... [8]
Formatted ... [4]
Formatted ... [9]
Formatted ... [10]
Deleted: (rapid[b])
Formatted ... [6]
Formatted ... [11]
Formatted ... [15]
Deleted: 82
Formatted ... [20]
Formatted ... [12]
Formatted ... [13]
Formatted ... [14]
Formatted ... [16]
Formatted ... [17]
Formatted ... [18]
Deleted: 2
Deleted: 034
Formatted ... [19]
Deleted: 82
Formatted ... [27]
Formatted ... [28]
Deleted: 233
Formatted ... [21]
Formatted ... [22]
Formatted ... [23]
Formatted ... [24]
Formatted ... [25]
Formatted ... [29]
Formatted ... [26]
Formatted ... [30]
Formatted ... [31]
Formatted ... [32]
Formatted ... [33]
Deleted: 78
Formatted ... [34]
Formatted ... [35]
Formatted ... [36]
Formatted ... [37]
Deleted: 094
Formatted ... [38]
Formatted ... [39]
Formatted ... [40]
Formatted ... [41]
Formatted ... [42]
Deleted: 50
Formatted ... [43]
Formatted ... [44]
Formatted ... [45]

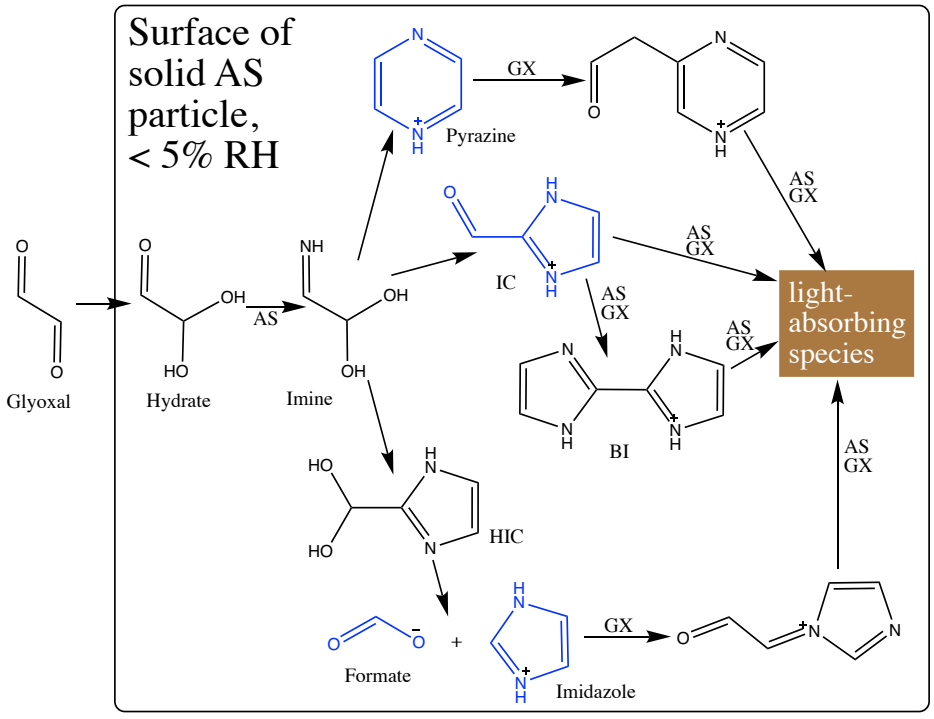

Scheme 1: Proposed brown carbon formation pathways of glyoxal reacting at solid AS aerosol particle surfaces. Products detected in this study are shown in blue. IC = 1H-imidazole-2-carboxaldehyde. BI = 2,2'-biimidazole (Kampf et al., 2012). AS = ammonium sulfate. GX = glyoxal. We assume, following (Kampf et al., 2012), that all reactions are reversible except for formation of N-heterocycle rings. See Scheme S1 for corresponding diagram of pathways under conditions of humidification.

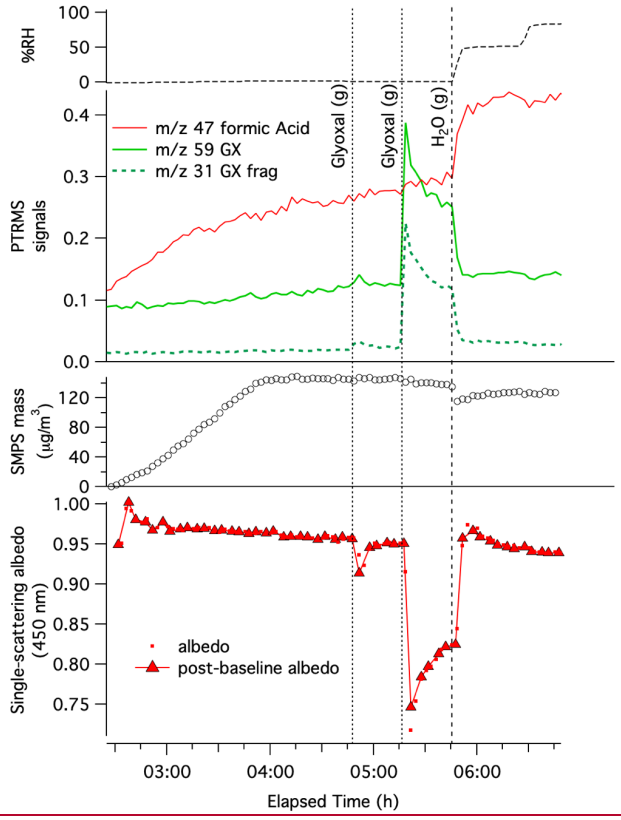

Figure 1: Pulse glyoxal addition experiment 1 on dry AS aerosol in CESAM chamber. Top: chamber RH. Middle panels: Dilution- and water-corrected PTR-MS traces for gas-phase glyoxal (*m/z* = 59, green line), a glyoxal fragment (*m/z* 31, dark green dotted line), formic acid (*m/z* 47, red line); SMPS particulate mass corrected for wall losses and dilution (assuming aerosol density = 1.77 g/cm^3, open black circles), with increasing mass for first 90 minutes indicating AS aerosol addition to chamber. Bottom: single-scattering albedo (red dots), and albedo values calculated from data immediately following instrument baseline on gas-phase contents of chamber (red triangles), measured by CAPS-ssa at 450 nm. Sequential gas "(g)" additions of 0.05 and 0.50 ppm glyoxal (vertical dotted line) and water vapor addition (dashed lines) are labeled. Elapsed time is measured from start of N_2 addition to the evacuated chamber.

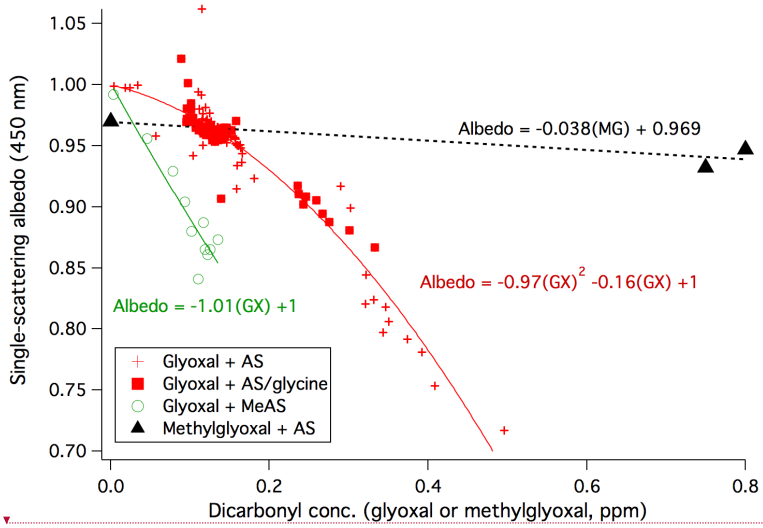

Figure 2: Top: Anticorrelation of particle single-scattering albedo at 450 nm (with a 3 – 7 min delay) with gas-phase concentrations of glyoxal (Expts. 1, 3, and 4: dry AS, red +; Expt. 2: dry AS/glycine, filled red squares; Expt. 5: dry MeAS, green circles) and methylglyoxal (black triangles, from (De Haan et al., 2017)) as measured by PTR-MS (expts. 1-2 and methylglyoxal data) or photoacoustic spectroscopy (expts. 3-5).

Deleted: ¶
¶

Deleted: 8

Deleted: ref

Deleted: 4, 8

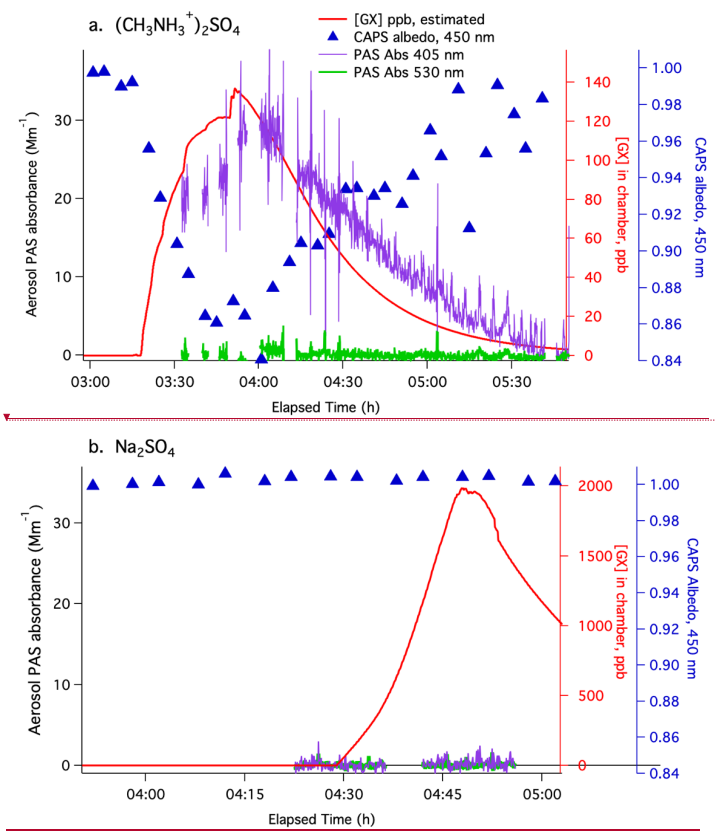

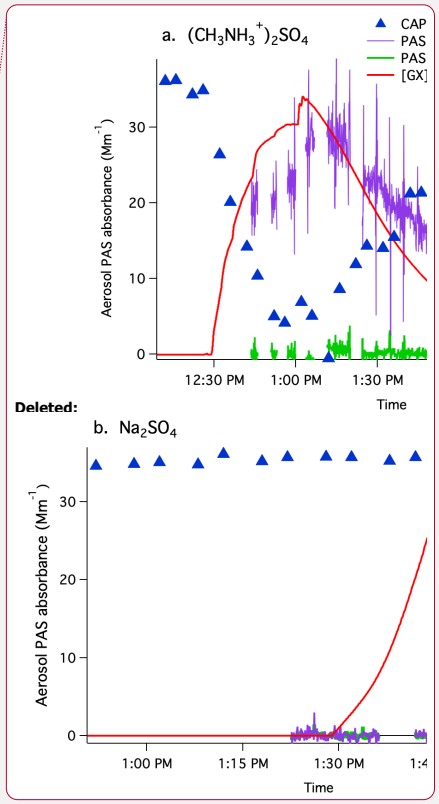

Figure 3: Gradual glyoxal addition experiments in small Tedlar chamber on **a.**) dry methylammonium sulfate aerosol (experiment 5), and **b.**) dry sodium sulfate aerosol (experiment 6). Aerosol absorbance measured by PAS at 405 nm (purple lines) and 530 nm (green lines), aerosol albedo measured by CAPS at 450 nm (blue triangles, blue axis), and estimated glyoxal concentrations in the chamber (red line, red axis, calculated using GX measurements at inlet, flow mixing ratios, and GX wall loss rate = 6.7×10^{-4} s^{-1}). CRD, SMPS, and 405 nm albedo data for these experiments is displayed in Figures S3 and S4, respectively.

Deleted: 8

Deleted: 9

Deleted: line

Deleted: line

Formatted: Indent: Left: 0", Hanging: 0.25"

Page 29: [1] Formatted **David De Haan** **6/9/20 7:20:00 PM**

Left, Line spacing: single, Position: Horizontal: Left, Relative to: Column, Vertical: In line, Relative to: Margin, Horizontal: 0", Wrap Around

Page 29: [2] Formatted Table **David De Haan** **6/9/20 7:20:00 PM**

Formatted Table

Page 29: [3] Formatted **David De Haan** **6/9/20 7:20:00 PM**

Font: 12 pt

Page 29: [4] Formatted **David De Haan** **6/9/20 7:20:00 PM**

Font: 12 pt

Page 29: [5] Formatted **David De Haan** **6/9/20 7:20:00 PM**

Font: 12 pt

Page 29: [6] Formatted **David De Haan** **6/9/20 7:20:00 PM**

Font: 12 pt

Page 29: [7] Inserted Cells **David De Haan** **6/9/20 7:20:00 PM**

Inserted Cells

Page 29: [8] Formatted **David De Haan** **6/9/20 7:20:00 PM**

Left, Line spacing: single, Position: Horizontal: Left, Relative to: Column, Vertical: In line, Relative to: Margin, Horizontal: 0", Wrap Around

Page 29: [9] Formatted **David De Haan** **6/9/20 7:20:00 PM**

Font: 12 pt

Page 29: [10] Formatted **David De Haan** **6/9/20 7:20:00 PM**

Font: 12 pt

Page 29: [11] Formatted **David De Haan** **6/9/20 7:20:00 PM**

Font: 12 pt

Page 29: [12] Formatted **David De Haan** **6/9/20 7:20:00 PM**

Position: Horizontal: Left, Relative to: Column, Vertical: In line, Relative to: Margin, Horizontal: 0", Wrap Around

Page 29: [13] Formatted **David De Haan** **6/9/20 7:20:00 PM**

Font: 12 pt

Page 29: [14] Formatted **David De Haan** **6/9/20 7:20:00 PM**

Font: 12 pt

Page 29: [15] Formatted **David De Haan** **6/9/20 7:20:00 PM**

Font: 12 pt

Page 29: [17] Formatted **David De Haan** **6/9/20 7:20:00 PM**

Position: Horizontal: Left, Relative to: Column, Vertical: In line, Relative to: Margin, Horizontal: 0", Wrap Around

Page 29: [18] Formatted **David De Haan** **6/9/20 7:20:00 PM**

Font: 12 pt

Page 29: [19] Formatted **David De Haan** **6/9/20 7:20:00 PM**

Font: 12 pt

Page 29: [20] Formatted **David De Haan** **6/9/20 7:20:00 PM**

Font: 12 pt

Page 29: [21] Formatted **David De Haan** **6/9/20 7:20:00 PM**

Position: Horizontal: Left, Relative to: Column, Vertical: In line, Relative to: Margin, Horizontal: 0", Wrap Around

Page 29: [22] Formatted **David De Haan** **6/9/20 7:20:00 PM**

Font: 12 pt

Page 29: [23] Formatted **David De Haan** **6/9/20 7:20:00 PM**

Font: 12 pt

Page 29: [24] Formatted **David De Haan** **6/9/20 7:20:00 PM**

Font: 12 pt

Page 29: [25] Formatted **David De Haan** **6/9/20 7:20:00 PM**

Font: 12 pt

Page 29: [26] Formatted **David De Haan** **6/9/20 7:20:00 PM**

Position: Horizontal: Left, Relative to: Column, Vertical: In line, Relative to: Margin, Horizontal: 0", Wrap Around

Page 29: [27] Formatted **David De Haan** **6/9/20 7:20:00 PM**

Font: 12 pt

Page 29: [28] Formatted **David De Haan** **6/9/20 7:20:00 PM**

Font: 12 pt

Page 29: [29] Formatted **David De Haan** **6/9/20 7:20:00 PM**

Font: 12 pt

Page 29: [30] Formatted **David De Haan** **6/9/20 7:20:00 PM**

Position: Horizontal: Left, Relative to: Column, Vertical: In line, Relative to: Margin, Horizontal: 0", Wrap Around

Page 29: [31] Formatted **David De Haan** **6/9/20 7:20:00 PM**

Font: 12 pt

Page 29: [33] Formatted **David De Haan** **6/9/20 7:20:00 PM**

Font: 12 pt

Page 29: [34] Formatted **David De Haan** **6/9/20 7:20:00 PM**

Font: 12 pt

Page 29: [35] Formatted **David De Haan** **6/9/20 7:20:00 PM**

Position: Horizontal: Left, Relative to: Column, Vertical: In line, Relative to: Margin, Horizontal: 0", Wrap Around

Page 29: [36] Formatted **David De Haan** **6/9/20 7:20:00 PM**

Font: 12 pt

Page 29: [37] Formatted **David De Haan** **6/9/20 7:20:00 PM**

Font: 12 pt

Page 29: [38] Formatted **David De Haan** **6/9/20 7:20:00 PM**

Font: 12 pt

Page 29: [39] Formatted **David De Haan** **6/9/20 7:20:00 PM**

Position: Horizontal: Left, Relative to: Column, Vertical: In line, Relative to: Margin, Horizontal: 0", Wrap Around

Page 29: [40] Formatted **David De Haan** **6/9/20 7:20:00 PM**

Font: 12 pt, Not Superscript/ Subscript

Page 29: [41] Formatted **David De Haan** **6/9/20 7:20:00 PM**

Font: 12 pt, Font color: Auto, Not Superscript/ Subscript

Page 29: [42] Formatted **David De Haan** **6/9/20 7:20:00 PM**

Font: 12 pt

Page 29: [43] Formatted **David De Haan** **6/9/20 7:20:00 PM**

Font: 12 pt, Not Superscript/ Subscript

Page 29: [44] Formatted **David De Haan** **6/9/20 7:20:00 PM**

Position: Horizontal: Left, Relative to: Column, Vertical: In line, Relative to: Margin, Horizontal: 0", Wrap Around

Page 29: [45] Formatted **David De Haan** **6/9/20 7:20:00 PM**

Font: 12 pt

Page 29: [46] Formatted **David De Haan** **6/9/20 7:20:00 PM**

Font: 12 pt, Not Superscript/ Subscript

Page 29: [47] Formatted **David De Haan** **6/9/20 7:20:00 PM**

Font: 12 pt

Page 29: [49] Formatted **David De Haan** **6/9/20 7:20:00 PM**

Font: 12 pt, Not Superscript/ Subscript

Page 29: [50] Formatted **David De Haan** **6/9/20 7:20:00 PM**

Font: 12 pt, Font color: Auto

Page 29: [51] Formatted **David De Haan** **6/9/20 7:20:00 PM**

Font: 12 pt

Page 29: [52] Formatted **David De Haan** **6/9/20 7:20:00 PM**

Font: 12 pt

Page 29: [53] Formatted **David De Haan** **6/9/20 7:20:00 PM**

Position: Horizontal: Left, Relative to: Column, Vertical: In line, Relative to: Margin, Horizontal: 0", Wrap Around

Page 29: [54] Formatted **David De Haan** **6/9/20 7:20:00 PM**

Font: 12 pt

Page 29: [55] Formatted **David De Haan** **6/9/20 7:20:00 PM**

Font: 12 pt

Page 29: [56] Formatted **David De Haan** **6/9/20 7:20:00 PM**

Font: 12 pt

Page 29: [57] Formatted **David De Haan** **6/9/20 7:20:00 PM**

Position: Horizontal: Left, Relative to: Column, Vertical: In line, Relative to: Margin, Horizontal: 0", Wrap Around

Page 29: [58] Formatted **David De Haan** **6/9/20 7:20:00 PM**

Font: 12 pt

Page 29: [59] Formatted **David De Haan** **6/9/20 7:20:00 PM**

Font: 12 pt, Font color: Auto

Page 29: [60] Formatted **David De Haan** **6/9/20 7:20:00 PM**

Font: 12 pt, Not Highlight

Page 29: [61] Formatted **David De Haan** **6/9/20 7:20:00 PM**

Font: 12 pt

Page 29: [62] Formatted **David De Haan** **6/9/20 7:20:00 PM**

Font: 12 pt

Page 29: [63] Inserted Cells **David De Haan** **6/9/20 7:20:00 PM**

Inserted Cells

Page 29: [64] Formatted **David De Haan** **6/9/20 7:20:00 PM**

Page 29: [65] Formatted **David De Haan** **6/9/20 7:20:00 PM**

Font: 12 pt

Page 29: [66] Formatted **David De Haan** **6/9/20 7:20:00 PM**

Font: 12 pt

Page 29: [67] Formatted **David De Haan** **6/9/20 7:20:00 PM**

Position: Horizontal: Left, Relative to: Column, Vertical: In line, Relative to: Margin, Horizontal: 0", Wrap Around

Page 29: [68] Formatted **David De Haan** **6/9/20 7:20:00 PM**

Font: 12 pt, Not Superscript/ Subscript

Page 29: [69] Formatted **David De Haan** **6/9/20 7:20:00 PM**

Font: 12 pt, Font color: Auto, Not Superscript/ Subscript

Page 29: [70] Formatted **David De Haan** **6/9/20 7:20:00 PM**

Font: 12 pt

Page 29: [71] Formatted **David De Haan** **6/9/20 7:20:00 PM**

Font: 12 pt, Not Superscript/ Subscript

Page 29: [72] Formatted **David De Haan** **6/9/20 7:20:00 PM**

Font: 12 pt

Page 29: [73] Formatted **David De Haan** **6/9/20 7:20:00 PM**

Position: Horizontal: Left, Relative to: Column, Vertical: In line, Relative to: Margin, Horizontal: 0", Wrap Around

Page 29: [74] Formatted **David De Haan** **6/9/20 7:20:00 PM**

Font: 12 pt

Page 29: [75] Deleted **David De Haan** **6/9/20 7:20:00 PM**

Page 29: [75] Deleted **David De Haan** **6/9/20 7:20:00 PM**

Page 29: [76] Formatted **David De Haan** **6/9/20 7:20:00 PM**

Font: 12 pt

Page 29: [77] Formatted **David De Haan** **6/9/20 7:20:00 PM**

Position: Horizontal: Left, Relative to: Column, Vertical: In line, Relative to: Margin, Horizontal: 0", Wrap Around

Page 29: [78] Formatted **David De Haan** **6/9/20 7:20:00 PM**

Font: 12 pt

Page 29: [79] Deleted **David De Haan** **6/9/20 7:20:00 PM**

Page 29: [79] Deleted **David De Haan** **6/9/20 7:20:00 PM**

Page 29: [80] Formatted **David De Haan** **6/9/20 7:20:00 PM**

Font: 12 pt, Font color: Auto, Not Superscript/ Subscript

Page 29: [81] Formatted **David De Haan** **6/9/20 7:20:00 PM**

Font: 12 pt

Page 29: [82] Formatted **David De Haan** **6/9/20 7:20:00 PM**

Font: 12 pt

Page 29: [83] Formatted **David De Haan** **6/9/20 7:20:00 PM**

Font: 12 pt

Page 29: [84] Formatted **David De Haan** **6/9/20 7:20:00 PM**

Position: Horizontal: Left, Relative to: Column, Vertical: In line, Relative to: Margin, Horizontal: 0", Wrap Around

Page 29: [85] Formatted **David De Haan** **6/9/20 7:20:00 PM**

Font: 12 pt

Page 29: [86] Formatted **David De Haan** **6/9/20 7:20:00 PM**

Font: 12 pt

Page 29: [87] Formatted **David De Haan** **6/9/20 7:20:00 PM**

Position: Horizontal: Left, Relative to: Column, Vertical: In line, Relative to: Margin, Horizontal: 0", Wrap Around

Page 29: [88] Formatted **David De Haan** **6/9/20 7:20:00 PM**

Font: 12 pt, Not Superscript/ Subscript

Page 29: [89] Formatted **David De Haan** **6/9/20 7:20:00 PM**

Font: 12 pt, Font color: Auto, Not Superscript/ Subscript

Page 29: [90] Formatted **David De Haan** **6/9/20 7:20:00 PM**

Font: 12 pt

Page 29: [91] Formatted **David De Haan** **6/9/20 7:20:00 PM**

Font: 12 pt, Not Superscript/ Subscript

Page 29: [92] Formatted **David De Haan** **6/9/20 7:20:00 PM**

Font: 12 pt

Page 29: [93] Formatted **David De Haan** **6/9/20 7:20:00 PM**

Position: Horizontal: Left, Relative to: Column, Vertical: In line, Relative to: Margin, Horizontal: 0", Wrap Around

Page 29: [94] Formatted **David De Haan** **6/9/20 7:20:00 PM**

Page 29: [95] Formatted **David De Haan** **6/9/20 7:20:00 PM**

Font: 12 pt

Page 29: [96] Formatted **David De Haan** **6/9/20 7:20:00 PM**

Position: Horizontal: Left, Relative to: Column, Vertical: In line, Relative to: Margin, Horizontal: 0", Wrap Around

Page 29: [97] Formatted **David De Haan** **6/9/20 7:20:00 PM**

Font: 12 pt, Not Superscript/ Subscript

Page 29: [98] Formatted **David De Haan** **6/9/20 7:20:00 PM**

Font: 12 pt, Font color: Auto

Page 29: [99] Formatted **David De Haan** **6/9/20 7:20:00 PM**

Font: 12 pt

Page 29: [100] Formatted **David De Haan** **6/9/20 7:20:00 PM**

Font: 12 pt, Not Superscript/ Subscript

Page 29: [101] Formatted **David De Haan** **6/9/20 7:20:00 PM**

Font: 12 pt

Page 29: [102] Formatted **David De Haan** **6/9/20 7:20:00 PM**

Position: Horizontal: Left, Relative to: Column, Vertical: In line, Relative to: Margin, Horizontal: 0", Wrap Around

Page 29: [103] Formatted **David De Haan** **6/9/20 7:20:00 PM**

Font: 12 pt

Page 29: [104] Formatted **David De Haan** **6/9/20 7:20:00 PM**

Font: 12 pt

Page 29: [105] Deleted **David De Haan** **6/9/20 7:20:00 PM**